Protein disulfide isomerase inhibition synergistically enhances the efficacy of sorafenib for hepatocellular carcinoma

Jae-Kyung Won[1, 2, 3, §], Su Jong Yu[4, §], Chae Young Hwang[1, §], Sung-Hwan Cho[1], Sang-Min Park[1], Kwangsoo Kim[5], Won-Mook Choi[4], Hyeki Cho[4], Eun Ju Cho[4], Jeong-Hoon Lee[4], Kyung Bun Lee[3], Yoon Jun Kim[4], Kyung-Suk Suh[6], Ja-June Jang[3], Chung Yong Kim[4], Jung-Hwan Yoon[4, *], Kwang-Hyun Cho[1,2, *]

[1]*Laboratory for Systems Biology and Bio-inspired Engineering, Department of Bio and Brain Engineering, Korea Advanced Institute of Science and Technology (KAIST), Daejeon 34141, Korea*

[2]*Graduate School of Medical Science and Engineering, KAIST, Daejeon 34141, Korea*

[3]*Department of Pathology, Seoul National University Hospital, Seoul National University College of Medicine, Seoul 110-744, Korea*

[4]*Department of Internal Medicine and Liver Research Institute, Seoul National University College of Medicine, Seoul 110-744, Korea*

[5]*Division of Clinical Bioinformatics, Biomedical Research Institute, Seoul National University Hospital, Seoul 110-744, Korea*

[6]*Department of Surgery, Seoul National University Hospital, Seoul National University College of Medicine, Seoul 110-744, Korea*

This article has been accepted for publication and undergone full peer review but has not been through the copyediting, typesetting, pagination and proofreading process which may lead to differences between this version and the Version of Record. Please cite this article as doi: 10.1002/hep.29237

Keywords: PDI, sorafenib, HCC, ER stress, combination therapy

§ J.-K. Won, S. J. Yu and C. Y. H. equally contributed to this work.

* J.-H. Yoon and K.-H. Cho equally contributed to this work.

Corresponding author:

Prof. Kwang-Hyun Cho

Department of Bio and Brain Engineering,

Korea Advanced Institute of Science and Technology (KAIST),

Daejeon 34141, Republic of Korea

Fax number: 82-42-350-4310, *Phone number*: 82-42-350-4325

E-mail address: ckh@kaist.ac.kr

Abbreviations

PDI, protein disulfide isomerase;

HCC, hepatocellular carcinoma;

ER stress, endoplasmic reticulum stress

UPR, unfolded protein response

ERAD, ER-associated degradation

HSP, heat shock protein

RT-PCR, reverse-transcription PCR

qRT-PCR, quantitative real-time PCR

BCLC, Barcelona Clinic Liver Cancer ;

mRECIST, modified Response Evaluation Criteria in Solid Tumors;

CR, complete response; PR, partial response; SD, stable disease; PD, progressive disease; DCR, disease control rate;

IHC, immunohistochemistry;

ROC, receiver-operating characteristic;

TTP, Time to progression; OS, overall survival;

Conflict of interest:

The authors who have participated in this study declared that they do not have anything to disclose regarding funding or conflict of interest with respect to this manuscript. But the authors below would like to disclose the following interest.

Jung-Hwan Yoon: Has received a research grant from Bayer HealthCare Pharmaceuticals

Yoon Jun Kim: Has received research grants from Bristol-Myers Squibb, Roche, JW Creagene, Bukwang Pharmaceuticals, Handok Pharmaceuticals, Hanmi Pharmaceuticals, Yuhan Pharmaceuticals, and Pharmaking, and has received lecture fees from Bayer HealthCare Pharmaceuticals, Gilead Science, MSD Korea, Yuhan Pharmaceuticals, Samil Pharmaceuticals, CJ Pharmaceuticals, Bukwang Pharmaceuticals, and Handok Pharmaceuticals

Su Jong Yu: Has received a lecture fee from Bayer HealthCare Pharmaceuticals. The remaining authors disclose no conflict.

Financial support:

This work was supported by the National Research Foundation of Korea (NRF) grants funded by the Korea Government, the Ministry of Science, ICT & Future

Planning (2015M3A9A7067220, 2014R1A2A1A10052404, 2013M3C8A1078501 and 2013M3A9A7046303) and a grant of the Korea Health Technology R&D Project through the Korea Health Industry Development Institute (KHIDI), funded by the Ministry of Health & Welfare, Republic of Korea (HI14C1277). It was also supported by grants from the SNUH Research Fund (No. 03-2012-0390) and the Liver Research Foundation of Korea.

Abstract

Sorafenib is the only approved targeted drug for hepatocellular carcinoma (HCC), but its effect on patients' survival gain is limited and varies over a wide range depending on patho-genetic conditions. Thus, enhancing the efficacy of sorafenib and finding a reliable predictive biomarker are crucial to achieve efficient control of HCCs. In this study, we employed a systems approach by combining transcriptome analysis of the mRNA changes in HCC cell lines in response to sorafenib with network analysis to investigate the action and resistance mechanism of sorafenib. Gene list functional enrichment analysis and gene set enrichment analysis (GSEA) revealed that proteotoxic stress and apoptosis modules are activated in the presence of sorafenib. Further analysis of the endoplasmic reticulum (ER) stress network model combined with *in vitro* experiments showed that introducing an additional stress by treating the orally active protein disulfide isomerase (PDI) inhibitor (PACMA 31) can synergistically increase the efficacy of sorafenib *in vitro* and *in vivo*, which was confirmed using a mouse xenograft model. We also found that HCC patients with high PDI expression show resistance to sorafenib and poor clinical outcomes, compared to the low PDI expression group.

Conclusion: These results suggest that PDI is a promising therapeutic target for enhancing the efficacy of sorafenib and can also be a biomarker for predicting sorafenib responsiveness.

Sorafenib, the first oral multi-kinase inhibitor, was approved for the treatment of hepatocellular carcinoma (HCC) a few years ago, but it has shown limited efficacy. Only a small fraction of patients (about 10%) show a clinical response to sorafenib and at most 30-40% of HCC patients demonstrate a disease control rate (1). In SHARP trial, the median survival period was prolonged by sorafenib up to three months, but its benefit is not enough considering its high price and varying efficacy depending on patients (2).

In general, targeted anti-cancer drug should have a biomarker to predict its clinical response. Single kinase inhibitors such as tarceva (EGFR inhibitor) or crizotinib (ALK inhibitor) have the predictive markers like EGFR mutation and ALK translocation, respectively. However, such markers are still not available for sorafenib since it targets multiple kinases including BRAF, VEGFR2, PDGFR, FLT3, RET and c-KIT, complicating the mechanism of action (3). Thus, it is clinically important to investigate the mechanism of resistance to sorafenib and develop a new therapeutic strategy that can improve the efficacy of sorafenib.

To discover the action and resistance mechanism of sorafenib, we adopted systems approaches as follows: First, we analyzed mRNA expression changes in HCC cell lines in response to sorafenib and inferred that ER stress pathway contributes to apoptosis driven by sorafenib. Second, based on these pathways, we constructed a network model and identified an apoptosis-promoting module as well as anti-apoptotic modules upon sorafenib treatment. Then, using the network kernel analysis and *in silico* simulation based on the logic diagram and a computational model, we found that PDI can be a therapeutic target for enhancing the efficacy of sorafenib.

We further unveiled that the combinatorial treatment of sorafenib and PDI inhibitor shows a synergistic effect *in vitro* and *in vivo.* In addition, we found that high PDI expression indicates a poor response rate to sorafenib treatment and adverse clinical outcomes in the HCC patients cohort.

Taken together, these results suggest that PDI can be not only a useful predictive biomarker for sorafenib, but also a promising target for the combination therapy to overcome the resistance to sorafenib.

Materials and Methods

mRNA microarray experiments and analysis

mRNA microarray experiments were performed in triplicate. HCC cell lines (SNU761, Huh7, Hep3B and HepG2) was treated with sorafenib 3 μM for 24 hours, while the control group was treated with only DMSO. Experiments were performed as described in Supporting Information.

HCC cell lines and cell culture

Human HCC cell lines Hep3B, SNU475, SNU761, HepG2, and Huh7 cells were cultured in Dulbecco's modified Eagle's medium (WelGENE Inc., Republic of Korea) with 10% fetal bovine serum (FBS) and antibiotics (100 units/ml of penicillin, 100 ug/ml streptomycin and 0.25 μg/ml of Fungizone) (Life Technologies Corp., Carlsbad, CA) at 37°C in a humidified atmosphere containing 5% CO_2.

Reagents

Sorafenib tosylate was purchased from LC Laboratories (Woburn, MA). Dimethyl sulfoxide (DMSO), thapsigargin, and propidium iodide (PI) were purchased from Sigma-Aldrich (Saint Louis, MO). PACMA 31 was purchased from Tocris Bioscience (Bristol, UK). Bortezomib was purchased from Selleck Chemicals (MA).

Western blot analysis

Cells were lysed in lysis buffer (20 mM HEPES, pH 7.2, 150 mM NaCl, 0.5% Triton X-100, 10% glycerol, 1 μg/ml aprotinin, 1 μg leupeptin, 1 mM Na_3VO_4, 1 mM NaF). Cell lysates were centrifuged at 13,000 rpm for 15 minutes at 4°C, and the resulting supernatants followed by SDS-PAGE and immunoblot analysis. For immunoblotting, anti-phospho-eIF2a (Cell Signaling Technology, Danvers, MA), anti-PDI (Invitrogen, Carlsbad, CA) and anti-α-actinin (Santa Cruz Biotechnology, Inc., Dallas, TX) were used. The rabbit polyclonal anti-GAPDH antibody was a generous gift from Dr. Ki-Sun Kwon (Korea Research Institute of Bioscience and Biotechnology).

Reverse transcription (RT)-PCR and* quantitative real-time (*qRT)-PCR

Total RNA was extracted from cultured cells with RNA-spin™ (iNtRON, Republic of Korea) and subjected to RT-PCR analysis. RT-PCR was performed using DiaStar™ RT kit (Solgent, Republic of Korea) and 2X Taq Premix (Solgent) with the following primers for human: CHOP Forward-1, 5'- TGT CAG CTG GGA GCT GGA AGC -3'; CHOP Forward-2, 5'- ACT CTT GAC CCT GCT TCT CTG -3'; CHOP Reverse, 5'-ATT CGG TCA ATC AGA GCT CGG -3'; β-actin Forward, 5'-AGA GCT ACG AGC TGC CTG AC-3'; β-actin Reverse, 5'-AGC ACT GTG TTG GCG TAC AG-3'. GAPDH Forward, 5'-CGC TCT CTG CTC CTC CTG TT-3'; GAPDH Reverse, 5'-CCA TGG

TGT CTG AGC GAT GT-3'. qPCR analysis was performed using the StepOnePlus (Applied Biosystems, Waltham, MA) with a 20 μL reaction volume containing cDNA, primers, and SYBR Master Mix (Applied Biosystems). The data were normalized against GAPDH mRNA in each reaction.

Pathway-focused gene expression profiling (PCR-based array)

Pathway-focused gene expression profiling was done using a 96-well human unfolded protein response PCR Array, RT^2 Profiler PCR array (PAHS-089Z, Human Unfolded Protein Response RT^2 Profiler PCR Array, Qiagen). In this array, 84 wells contained all the components required for the PCR reaction in addition to a primer for a single gene in each well. These genes are involved in unfolded protein binding, ER protein folding quality control, regulation of cholesterol metabolism, regulation of translation, endoplasmic reticulum associated degradation (ERAD), ubiquitination, transcription factors, protein folding, protein disulfide isomerization, heat shock proteins, and apoptosis. A diluted cDNA template was mixed with the RT^2 SYBR® green master mix (Qiagen) according to the manufacture's protocol and loaded onto the 96-well array plate. qPCR analysis was performed using the QuantStudio 5 (Applied Biosystems), by heating the plate to 95 °C for 10 min, followed by 40 cycles of 95 °C for 15 seconds and 60 °C for 1 minutes. The data were normalized, across all plates, to the following housekeeping genes: hypoxanthine phosphoribosyltransferase 1 (HPRT1), beta-2-microglobulin (B2M), ribosomal protein, large, P0 (RPLP0) glyceraldehydes-3-phosphate dehydrogenase (GAPDH), and β-actin.

Plasmid Construction, Virus Production, and Infection

For lentivirus production, HEK 293T cells were transfected with relevant *lentiviral plasmid* and packaging mix (pLP1, pLP2 and pLP/VSVG) using Lipofectamine (Invitrogene) according to the manufacturer's instructions. For overexpression experiments, the full-length cDNA of PDI was amplified by RT–PCR from total RNA isolated from SNU761 cells using PCR amplification with a forward primer containing *Xba*I site (5′- TCCGTGTCTAGAATGCTGCGCCGCGCTCTG-3′) and a reverse primer containing *EcoR*I site (5′- TGGCTTGAATTCTTACAGTTCATCTTTCACAG-3′). The PCR fragment was digested by *Xba*I and *EcoR*I, ligated into the pLentiM1.4 lentiviral vector, and confirmed by sequencing. For CHOP knockdown, the plasmid encoding shRNA targeting CHOP in pLKO.1 was used (Sigma-Aldrich).

Network kernel analysis

To investigate the core structure of a network, the kernel identification algorithm which condenses a biological network into a smaller one while preserving the input-output dynamics of a network and topological aspects, was adopted as previously described (4). This algorithm recursively replaces the neighborhood subnetwork of each node with a smaller network which has the same dynamics as the original network, until no further replacement is possible. It is known that essential genes, disease-associated genes and drug targets are enriched in the reduced kernel network (4).

The logic diagram and computational modeling of ER stress pathway

An ordinary differential equation (ODE)-based computational model was

constructed to investigate the effect of combination treatments. We have applied the step-function (θ) to describe the dynamic activities by logical approximation of ODE. Step-function is defined as follows.

$$\theta(x > T) = \begin{cases} 1, x > T \\ 0, x \le T \end{cases}$$

where T is the threshold for the node activation.

$$\frac{d[MP]}{dt} = k_1 Sorafenib(t) - k_2[MP],$$

$$\frac{d[ER]}{dt} = k_3[MP] - k_4[ER],$$

$$\frac{d[PDI, HSP]}{dt} = k_5(w_1[MP] + w_2[ATF6, IRE1] - w_3 PDI\_inhibitor(t)) - k_6[PDI, HSP],$$

$$\frac{d[ATF6, IRE1]}{dt} = k_7[ER] - k_8[ATF6, IRE1],$$

$$\frac{d[RMP]}{dt} = k_9[PDI, HSP] - k_{10}[RMP],$$

$$\frac{d[UPS]}{dt} = k_{11}(w_4[MP] - w_5[ATF6, IRE1] - w_6 Proteasome\_input(t) + w_7[PDI, HSP])\theta(w_4[MP] - w_5[ATF6, IRE1] - w_6 Proteasome\_inhibitor(t) > T_1)\theta([PDI, HSP] > T_2) - k_{12}[UPS],$$

$$\frac{d[CHOP]}{dt} = k_{13}(w_8[ER] - w_9[RMP] - w_{10}[UPS]) - k_{14}[CHOP],$$

$$\frac{d[Apoptosis]}{dt} = k_{15}[CHOP] - k_{16}[Apoptosis]$$

where [MP], [RMP] and [UPS] denote the misfolded proteins, refolding of misfolded proteins and ubiquitin-proteasome system, respectively, and k_1, k_2, k_3, k_4, k_5, k_6, k_7, k_8, k_9, k_{10}, k_{11}, k_{12}, k_{13}, k_{14}, k_{15}, and k_{16} denote the kinetic parameters, T_1 and T_2 represent the activation threshold of each node, w_1, w_2, w_3, w_4, w_5, w_6, w_7, w_8, w_9, and w_{10} represent the cooperation weights of each node activation, respectively. For the simulation results, we used k_1=0.2, k_2=0.2, k_3=0.3, k_4=0.3, k_5=0.3, k_6=0.2, k_7=0.2, k_8=0.2, k_9=0.2, k_{10}=0.2, k_{11}=0.14, k_{12}=0.2, k_{13}=0.2, k_{14}=0.2, k_{15}=0.2, k_{16}=0.2, w_1=0.3,

w_2=0.3, , w_3=0.3, w_4=1.5, w_5=1, w_6=0.3, w_7=0.3, w_8=0.8, w_9=0.9, w_{10}=0.5, T_1=0, and T_2=0.

Cell viability assays

HCC cells were seeded into 96-well plate at a density of 6 × 10^3 cells/well in growth medium, incubated for 24 or 48 hours and then treated with the indicated concentrations of sorafenib (LC Laboratories) and PACMA 31 (Tocris Bioscience), alone or in combination. Following incubation of the plates for 24 hours, relative cell viability was measured. Briefly, WST-1 solution (Daeillab, Republic of Korea) was added to cells for 30 minutes ~ 2 hours and then measured the absorbance at 450 nm using a xMark™ Microplate Absorbance Spectrophotometer (Bio-Rad, Hercules, CA).

Cell death assay

To analyze cell death, PI-based assays were performed. IncuCyte ZOOM (Essen Biosciences, Ann Arbor, MI) was used to detect cell death according to the manufacturer's instructions. HCC cells were seeded into 96-well plate and cultured for 24 hours (6 × 10^3 cells/well). Cells were then treated with the indicated concentrations of sorafenib (LC Laboratories) and PACMA 31 (Tocris Bioscience), alone or in combination for 24 hours. After seeding, cells were imaged using IncuCyte ZOOM (Essen Bioscience). To assess cell death, average areas of PI-labeled cells were determined at each time point using the IncuCyte ZOOM analysis software. Images were captured at 3 hours intervals from 3 separate regions per well with a 20 × objective.

Animals and treatments

Hep3B cells ($1x10^7$/100 μl) and BD matrigel 100 μl mixture (total 200 μl/head) were implanted subcutaneously into 5 week old female Balb/c nude mice. When the average volume of tumors reached 200 mm^3, the mice were randomly divided into 4 groups (*n*=8 per group) and then were orally treated with the vehicle (0.5% carboxymethylcellulose sodium, 10 mL/kg) or sorafenib (30 mg/kg) and PACMA 31 (20 mg/kg, intraperitoneal), alone or in combination once daily for 4 weeks. The tumor volume was calculated as $LxW^2/2$ (L: length; W: width) every 2 to 3 days. Mice were maintained on 12 hours dark/light cycle and fed standard chow. All animal experiments were conducted according to a protocol approved by the Institutional Animal Care and Committee of Seoul National University Hospital.

Eligibility criteria, treatment regimen and assessment of response to sorafenib in patients with HCC

The eligibility criteria for sorafenib therapy were (1) unresectable HCC according to the Barcelona clinic liver cancer (BCLC) staging classification [Hepatology 53:1020-2, 2011; J Hepatol 56:908-43, 2012]; (2) age < 80 years; (3) an Eastern Cooperative Group performance status of 0 or 1; (4) Child-Pugh grade A or B; (5) white blood cell count > 3,000 cells/mm^3 , hemoglobin level > 10 g/dL, platelet count >50,000 cells/mm^3; and (6) serum total bilirubin < 3.0 mg/dL, serum transaminases < 200 IU/L and serum creatinine < 1.5 mg/dL. These eligibility criteria were based on the vulnerability to adverse side effects. The diagnosis of HCC was confirmed based on hematoxylin–eosin staining of histopathological specimens in all patients. Sorafenib

was given orally at a dose of 400 mg twice daily. Treatment interruptions and up to two dose reductions (first to 400 mg once daily and then to 400 mg every 2 days) were permitted for drug-related adverse effects [the Common Terminology Criteria for Adverse Events (version 3)] (5). Treatment was continued until the radiologic progression, as defined by the modified Response Evaluation Criteria in Solid Tumors (mRECIST) (6). Assessed by contrast enhanced computed tomography or magnetic resonance imaging every 6-8 weeks, therapeutic response to sorafenib was defined according to the criteria of mRECIST. Complete response (CR) was defined as disappearance of all arterial-enhancing lesions. Partial response (PR) was defined as at least a 30% decrease in the sum of the longest diameter of viable target lesions, taking as reference the baseline sum of the diameters of target lesions. Progressive disease (PD) was defined as at least 20% increase in the sum of the diameters of viable target lesions, taking as reference the smallest sum of the diameters of viable target lesions recorded since treatment started. Stable disease (SD) was defined as any cases do not meet either PR or PD. When the response achieved for intrahepatic HCC differed from that for extrahepatic HCC, the worse response was determined as the achieved response. Assessment of response was introduced best overall response of mRECIST across all assessment time points.

Immunohistochemical analysis

Anti-PDI antibody (clone RL90) for IHC was purchased from Abcam (Cambridge, UK) and immunostaining was done using Ventana Optiview system (Roche Diagnositics, Mannheim, DE). Slides were scanned by Aperio ScanScope CS2 (Leica Biosystems, Nussloch, DE) and image files of each core were obtained. PDI

immunopositivity was calculated by the Positive Pixel Count Algorithm of the Aperio ImageScope (Leica Biosystems). Two or more cores per case were examined and the highest value was used as a representative value.

Statistical analysis

The Mann–Whitney U test and the Kruskal–Wallis test were used to analyze differences between the different groups. The Chi square test and Fisher's exact test were used for categorical data. To define the best cutoff value for predicting outcome, time-dependent receiver-operating characteristic (ROC) curves for censored survival data were constructed (7). The best cutoff value was adopted when it had the maximal sum of sensitivity and specificity. Time to progression (TTP) was calculated from the first day of sorafenib to PD. Overall survival (OS) was calculated from the date of commencement of sorafenib to the date of death or last contact. Conventional clinical factors at the time of entry into the study and immunopositivity for PDI were analyzed to identify variables that influenced survival as determined by the Kaplan-Meier method and compared by the log-rank test. Stepwise, multivariate analysis was performed using the Cox proportional hazards model to identify independent variables that influenced survival. Factors found to be significantly related to outcome by univariate analysis were included in the multivariate analysis. All statistical analyses were performed using SPSS version 19.0 (SPSS, Inc., Chicago, IL), and P values of <0.05 were considered significant.

Results

Sorafenib-responsive mRNA changes indicate that apoptosis can be induced

by proteotoxic stress from sorafenib

To identify the action mechanism and the resistance mechanism of sorafenib, the transcriptomic changes of HCC cell lines (SNU761, Huh7, Hep3B and HepG2) before and after sorafenib treatment were analyzed. Although their sensitivity to sorafenib was generally similar, SNU761 and Huh7 cells were relatively resistant to sorafenib compared to Hep3B and HepG2 cells (Supporting Fig. S1). To find out biologically relevant gene sets that significantly change, Gene list functional enrichment analysis and Gene Set Enrichment Analysis (GSEA) were done (Supporting Materials and Method).

It was shown that the unfolded protein response (UPR) gene set are significantly changed in SNU761, Huh7 and Hep3B, but to a lesser degree in HepG2 (Supporting File 1 and 2). This result raises the possibility that sorafenib causes proteotoxic stress which may lead to apoptosis or resistance in some groups of HCC cell lines.

To confirm this hypothesis, western blot for phospho-eIF2a, which is a marker of PERK axis activation, crucial in UPR, was conducted and it was shown that sorafenib induces UPR. In addition, RT-PCR of CHOP (DDIT3), which is known to be a marker for ER stress-induced apoptosis, suggests that ER stress-induced apoptosis might be brought about by sorafenib (Fig. 1). To confirm that hypothesis, cell viability assays of Hep3B cells expressing scrambled shRNA or CHOP shRNA were performed. Sorafenib-induced apoptosis was reduced in CHOP knockdown cells compared to control cells (Supporting Fig. S2).

The effect of sorafenib on ER stress network

To clarify the effect of sorafenib on ER stress pathway and to identify molecules that

can mitigate the efficacy of sorafenib and cause the resistance to apoptosis, we constructed a signaling network model of ER stress (Supporting Fig. S3). This network model is composed of three parts. One is the UPR part that is composed of UPR signal transducers being activated by the accumulation of unfolded or misfolded protein. The others are the protein refolding part and the ERAD part that relieve the proteotoxic stress by refolding or degrading misfolded proteins, which results in cell survival.

To explore this network, qRT-PCR-based array for 84 key molecules constituting this pathway was performed in SNU761 cell lines (Figure 2, Supporting Table S1). 37 out of 84 molecules were significantly upregulated when sorafenib was treated, whereas none was down-regulated (Supporting Table S1). When these changes were displayed on the network model, both the UPR and ERAD parts were found to be activated (Supporting Fig. S3). As seen in Figure 2, molecules for ER protein folding (Fig. 2C) and ubiquitin-proteasome pathway (Fig. 2D and 2E) were upregulated, which results in the resistance to apoptotic effects of sorafenib. To test whether this phenomenon occurs in another cell line, the same experiment was performed in HepG2 and Huh7 cell lines. HepG2 cell line was chosen because it showed a weaker unfolded protein response than other cell lines from microarray experiments, while Huh7 cell line showed similar responses with SNU761 cell line. As shown in Supporting Fig. S4, unfolded protein responses were not apparent in HepG2 cell line. But Huh7 cell line showed similar reactions with SNU761 cell line in qRT-PCR analysis (Supporting Fig. S5). These results suggests that ER stress is induced depending on cellular contexts.

Discovery of a target molecule for increasing the efficacy of sorafenib

To identify candidates for the combination therapy with sorafenib, two different approaches were used. First, we applied the kernel identification algorithm which elucidates essential nodes for network dynamics. The input set is the ER stress pathway network that consists of 20 nodes and 34 links (Supporting Fig. S6A). By the kernel identification algorithm, it was condensed into the smaller network with 6 nodes and 10 links (Supporting Fig. S6B). In this condensed network, heat shock proteins (HSPs) and PDI are found to be the crucial nodes against apoptosis. Because HSPs are the family of several molecules that cannot be completely blocked by one inhibitor, while PDI inhibitor can hinder the enzymatic activities of the broad ranges of PDI family, PDI was given the first priority as a target molecule.

Second, since the inhibition of proteasome by an inhibitor, such as bortezomib, has been known to cause proteotoxic stress and show synergistic effects with sorafenib (8), the comparison between the effect of proteasome inhibitor and that of PDI inhibitor was conducted *in silico* and *in vitro*. An ordinary differential equation model based on the logical approximation was constructed and the effect of each inhibitor was simulated (Fig. 3). As seen in Figure 3B, PDI inhibition shows much more synergy than proteasome inhibition and similar results were obtained with diverse coefficient values (Supporting Fig. S7).

To confirm those *in silico* results, cell viability assay and apoptosis assay were performed in multiple cell lines (Fig. 4). Whereas bortezomib demonstrated the mild additive effect with sorafenib (Supporting Fig. S8), PACMA 31 revealed the synergistic effects.

The effect of combined treatment with PACMA 31 on ER stress network

qRT-PCR-based array for 84 key molecules constituting ER stress network was performed (Fig. 5). While molecules intensifying apoptosis were up-regulated in the combination group (Fig. 5A and B), anti-apoptotic molecules such as XBP1 and MANF were down-regulated even in comparison with the control group. Molecules participating in protein folding and ERAD were down-regulated in the combination treatment group compared to the sorafenib group (Fig. 5C-F), except those that are involved in the activation of PDI (EDEM1 and ERO1L), while there were no such effects in PACMA 31 single treatment group. When these changes were displayed on the network model, we can find that ERAD part (right) and protein refolding (center) are turned off while the apoptotic pathway is activated in UPR part (Supporting Fig. S9).

In case of HepG2, UPR was not evident upon sorafenib treatment (Supporting Fig. S4) but synergistic cytotoxicity was observed with PACMA 31 like other cell lines (Fig. 4). As shown in Supporting Fig. S10, it was shown that JNK and CHOP are induced by the combinatorial treatment of sorafenib and PACMA 31.

The efficacy of the combined treatment with PACMA 31 *in vivo*

We further evaluated the effect of the combined treatment with PDI inhibitor using a xenograft mice model. As shown in Figure 6, the combined treatment significantly reduced tumor volume, while the others did not in comparison with the control group (two way repeated measure ANOVA $P<0.05$).

High PDI expression can predict a poor clinical outcome after sorafenib

treatment in patients with HCC

To find out the relationship between PDI expression and the clinical outcome in HCC patients receiving sorafenib, we analyzed the PDI immunopositivity in HCC patients who have been treated with sorafenib. Immunohistochemical analysis for PDI protein expression in our HCC patients cohort (*n*=95) demonstrated that PDI expression was increased in the tumor tissue of 59 cases (62.1%), whereas 36 cases (37.9%) showed the decrease of PDI expression compared to adjacent non-tumor tissue (Supporting Table S2). Among them, CR and PR were achieved in 2/95 (2.1%) and 1/95 (1.1%) of cases, respectively. SD was noted in 8/95 patients (8.4%) and disease control (CR + PR + SD) was achieved in 11/95 (11.6%). PD was noted in 84/95 (88.4%) of cases. The low PDI expression group showed a significantly better response (disease control) to sorafenib compared to the high PDI expression group (22.2% versus 5.1%, respectively; *P*=0.018) (Table 1). These results suggest that PDI might be involved in the response to sorafenib.

We then performed survival analysis. The median TTP was 2.2 months (range: 0.1–38.7 months). The cumulative progression-free survival rates at 3, 6 and 12 months were 40.8%, 19.7% and 6.6%, respectively. Forty-seven patients were alive at the end of the observation period, while 47 patients had died. The median survival time was 10.0 months (range: 1.0–76.0 months). The cumulative survival rate at 3, 6 and 12 months was 85.4%, 63.5% and 37.9%, respectively.

The impact of PDI expression in HCC tissues on the prognosis of patients treated with sorafenib was examined. As shown in Figure 7A, the Kaplan-Meier method demonstrated significant prolongation of TTP in the low PDI expression group, compared with the high PDI expression group (*P*=0.035). The prognostic factors for

TTP in multivariate analysis were high PDI expression [hazard ratio (HR) 1.833; 95% confidence interval (CI), 1.143–2.937; *P* = 0.012], age (HR 0.558; 95% CI, 0.339–0.918; *P* = 0.022), lymph node involvement (HR 2.368; 95% CI, 1.335–4.200; *P* = 0.003), and presence of metastasis (HR 3.478; 95% CI, 1.559–7.761; *P* = 0.002) (Supporting Table S3). A significant prolongation of OS in the low PDI expression group compared with the high PDI expression group (*P*=0.024; Figure 7B) was also found. The prognostic factors for OS in multivariate analysis were high PDI expression (HR 1.878; 95% CI, 1.107–3.184; *P* = 0.019), poor Child-Pugh score (HR 1.966; 95% CI, 1.349–2.864; *P* < 0.001), high number of tumors (HR 1.109; 95% CI, 1.037–1.186; *P* = 0.003), and lymph node involvement (HR 2.135; 95% CI, 1.148–3.971; *P* = 0.017) (Supporting Table S4).

Discussion

In this study, the gene expression changes upon sorafenib treatment were analyzed and it was found that proteotoxic stress and UPR are mainly associated with the resistance mechanism of sorafenib. Moreover, *in vitro* study showed that sorafenib brings about ER stress-induced apoptosis but its effect was attenuated by the activation of protein refolding and ERAD pathway. Network analysis and *in silico* simulation to discover a target molecule that can block those compensatory responses revealed that PDI can be a candidate. Further, *in vitro* and *in vivo* experiments proved that PDI inhibition shows the synergistic effect with sorafenib. We also found that PDI expression in HCC patients predicts the resistance to sorafenib treatment.

PDI is one of the most abundant soluble proteins in the ER and acts as a reductase,

an oxidase, and an isomerase as well as a molecular chaperone (9). The UPR is an important mechanism to sustain homeostasis between cell survival and apoptosis resulting from misfolded proteins (10, 11). Since PDI exerts key functions in protein folding, refolding and even retrotranslocation for ERAD (12), blocking this activity can be a way to hinder the mitigation of ER stress, which leads to cell death (13). Recent studies showed that PDI plays a crucial role in cancer survival and progression (14-16). In addition, it was reported that PDI mediates resistance to cytotoxic chemotherapy (17). In our previous work, the expression of PDI was increased in HCC compared to non-tumor tissue and high PDI expression level in HCC tissue adversely affected the clinical outcomes in HCC patients (18). The results of this study suggest that PDI exerts an important role in the the resistance to sorafenib. But when we performed PDI overexpression experiments in *in vitro*, it seems that PDI overexpression has little correlation with the response to sorafenib, but appears to make HCC cells more sensitive to the combination treatment of sorafenib and PDI inhibitor (Supporting Fig. 11). In addition to the low dosage of sorafenib in our study, some overexpression may not significantly affect the overall activity of PDI in *in vitro*, depending on cellular context, since PDI is an enzyme. In some cell lines, it has been shown that overexpression of PDI abrogated the effect of chemotherapeutic agents (17, 19). Maybe its effect will be diverse depending on drug dosage, cell types and cellular context. However, in *in vivo*, sorafenib has been known to induce tumor hypoxia through anti-angiogenic effect (20), which leads to more exposure to ER stress that is difficult to cope with (21). In this case, PDI overexpression can be helpful for cancer cells to survive. Indeed, in our patient cohort, high PDI expression in HCC tissues is significantly correlated with the sorafenib resistance and predicts

poor clinical outcomes after sorafenib treatment.

Cancer cells have developed several ways that can compensate stressful conditions (22). If we exploit those attributes, it will be possible to increase the vulnerability of cancer to anti-cancer drugs (19). In this study, we found that PDI can be a useful target.

In the course of searching a proper target molecule, we used two approaches: network kernel analysis and *in silico* simulations. First, network kernel analysis reduces the complex network to a simpler network while maintaining the original dynamics (4). As it has been known that the remaining genes in such a reduced network are enriched with drug targets and the synthetic lethal pairs, the reduced kernel network can be useful in searching for a potential target. Second, since it has been known that *in silico* simulations based on ODE modeling can be useful in the quantitative analysis of the effect of targeted inhibitor (23), we predicted that PDI inhibition can be more effective than proteasome inhibition from the simulation analysis. This might be because PDI is a hub node connecting the UPR part, protein refolding part and ERAD part. It should be noted that PDI plays multiple roles including the thiol-disulfide oxidoreductase, disulfide isomerase and molecular chaperone (24).

In the qRT-PCR experiment for ER stress network, some questions can be raised. Sorafenib increases overall expression of molecules belonging to UPR signal tranducer, chaperones and ERAD system in SNU761 and Huh7 cells. But when combined with PDI inhibitor, a majority of chaperones and ERAD proteins is downregulated together with anti-apoptotic molecules including XBP1 and MANF. The reason why such transcriptional effects occur remains as a challenging issue. In

our opinion, those expression changes might have been originated from CHOP induction by the combinatorial effect of sorafenib and PDI inhibition through uncompensated ER stress. Unfolded or misfolded client proteins can impose such ER stress, which leads to cell death in pathologic conditions. The transcription factor CHOP is activated by ER stress, and CHOP directly activates GADD34, which promotes ER client protein biosynthesis, but not ERAD or UPR proteins (25). Since endogenous reference genes of qRT-PCR analysis could be also included in the ER client proteins and might be induced by CHOP, it appears that UPR proteins including ERAD molecules seem to be relatively less expressed. It should be unveiled in future studies whether this phenomenon is caused by indirect effect through the uncompensated ER stress, or the combination treatment directly regulates these molecules by other pathways. In case of HepG2 cells, sorafenib alone seems to cause cell death in other ways without going through ER stress. However, when combined with PDI inhibitor, the expression of JNK and CHOP is highly increased (Supporting Fig. S10). Since JNK is also a well-known inducer of ER stress-induced apoptosis (26), it seems that the combination treatment enhances apoptosis in HepG2 cells through JNK-BCL2 axis unlike other cell lines. Further detailed mechanisms should be clarified in future studies.

In our patient cohort, PDI expression predicts the resistance to sorafenib and is significantly correlated with OS and TTP after sorafenib treatment. To verify this result, additional studies are needed using another patient cohorts and the relationship with other known resistance factors such as HIF-1α and VEGFR should be investigated (27, 28). And, testing a patient-derived xenograft model may be a valuable method to confirm the efficacy of the combination treatment with PDI

inhibitor.

In conclusion, PDI is an effective target for overcoming the resistance to sorafenib treatment and can also be a predictive marker to predict sorafenib responsiveness and clinical outcomes.

Acknowledgement

The pLentiM1.4 lentiviral vector was kindly provided by Dr. Y.-S. Kim (Chungnam National University, Daejeon, Korea). The authors thank Bo Hyun Kim for sharing her knowledge and ideas. The authors would like to thank Young Youn Cho, Sung-Hee Lee, Soo-Mi Lee and Hyo Ju Jang for their technical support and assistance in preparing this manuscript.

References

1. Kostner AH, Sorensen M, Olesen RK, Gronbaek H, Lassen U, Ladekarl M. Sorafenib in advanced hepatocellular carcinoma: a nationwide retrospective study of efficacy and tolerability. ScientificWorldJournal 2013;2013:931972.
2. Llovet JM, Ricci S, Mazzaferro V, Hilgard P, Gane E, Blanc JF, de Oliveira AC, et al. Sorafenib in advanced hepatocellular carcinoma. N Engl J Med 2008;359:378-390.
3. Cervello M, McCubrey JA, Cusimano A, Lampiasi N, Azzolina A, Montalto G. Targeted therapy for hepatocellular carcinoma: novel agents on the horizon. Oncotarget 2012;3:236-260.
4. Kim JR, Kim J, Kwon YK, Lee HY, Heslop-Harrison P, Cho KH. Reduction of complex signaling networks to a representative kernel. Sci Signal 2011;4:r

a35.

5. DCTD N, NIH, DHHS. Cancer Therapy Evaluation Program, Common Te rminology Criteria for Adverse Events (CTCAE). In. Version 3.0 ed; 2006.

6. Lencioni R, Llovet JM. Modified RECIST (mRECIST) assessment for hep atocellular carcinoma. Semin Liver Dis 2010;30:52-60.

7. Heagerty PJ, Lumley T, Pepe MS. Time-dependent ROC curves for cen sored survival data and a diagnostic marker. Biometrics 2000;56:337-344.

8. Chen KF, Yu HC, Liu TH, Lee SS, Chen PJ, Cheng AL. Synergistic inte ractions between sorafenib and bortezomib in hepatocellular carcinoma involve PP2A-dependent Akt inactivation. J Hepatol 2010;52:88-95.

9. Xu S, Sankar S, Neamati N. Protein disulfide isomerase: a promising ta rget for cancer therapy. Drug Discov Today 2014;19:222-240.

10. Walter P, Ron D. The unfolded protein response: from stress pathway to homeostatic regulation. Science 2011;334:1081-1086.

11. Hetz C. The unfolded protein response: controlling cell fate decisions un der ER stress and beyond. Nat Rev Mol Cell Biol 2012;13:89-102.

12. Vembar SS, Brodsky JL. One step at a time: endoplasmic reticulum-ass ociated degradation. Nat Rev Mol Cell Biol 2008;9:944-957.

13. Puig A, Lyles MM, Noiva R, Gilbert HF. The role of the thiol/disulfide ce nters and peptide binding site in the chaperone and anti-chaperone activities of protein disulfide isomerase. J Biol Chem 1994;269:19128-19135.

14. Higa A, Mulot A, Delom F, Bouchecareilh M, Nguyen DT, Boismenu D, Wise MJ, et al. Role of pro-oncogenic protein disulfide isomerase (PDI) family member anterior gradient 2 (AGR2) in the control of endoplasmic reticulum ho

meostasis. J Biol Chem 2011;286:44855-44868.

15. Tager M, Kroning H, Thiel U, Ansorge S. Membrane-bound proteindisulfide isomerase (PDI) is involved in regulation of surface expression of thiols and drug sensitivity of B-CLL cells. Exp Hematol 1997;25:601-607.

16. Goplen D, Wang J, Enger PO, Tysnes BB, Terzis AJ, Laerum OD, Bjerkvig R. Protein disulfide isomerase expression is related to the invasive properties of malignant glioma. Cancer Res 2006;66:9895-9902.

17. Tufo G, Jones AW, Wang Z, Hamelin J, Tajeddine N, Esposti DD, Martel C, et al. The protein disulfide isomerases PDIA4 and PDIA6 mediate resistance to cisplatin-induced cell death in lung adenocarcinoma. Cell Death Differ 2014;21:685-695.

18. Yu SJ, Won JK, Ryu HS, Choi WM, Cho H, Cho EJ, Lee JH, et al. A novel prognostic factor for hepatocellular carcinoma: protein disulfide isomerase. Korean J Intern Med 2014;29:580-587.

19. Lovat PE, Corazzari M, Armstrong JL, Martin S, Pagliarini V, Hill D, Brown AM, et al. Increasing melanoma cell death using inhibitors of protein disulfide isomerases to abrogate survival responses to endoplasmic reticulum stress. Cancer Res 2008;68:5363-5369.

20. Chang YS, Adnane J, Trail PA, Levy J, Henderson A, Xue D, Bortolon E, et al. Sorafenib (BAY 43-9006) inhibits tumor growth and vascularization and induces tumor apoptosis and hypoxia in RCC xenograft models. Cancer Chemother Pharmacol 2007;59:561-574.

21. Xu C, Bailly-Maitre B, Reed JC. Endoplasmic reticulum stress: cell life and death decisions. J Clin Invest 2005;115:2656-2664.

22. Hanahan D, Weinberg RA. Hallmarks of cancer: the next generation. Cell 2011;144:646-674.

23. Won JK, Yang HW, Shin SY, Lee JH, Heo WD, Cho KH. The crossregulation between ERK and PI3K signaling pathways determines the tumoricidal efficacy of MEK inhibitor. J Mol Cell Biol 2012;4:153-163.

24. Ali Khan H, Mutus B. Protein disulfide isomerase a multifunctional protein with multiple physiological roles. Front Chem 2014;2:70.

25. Marciniak SJ, Yun CY, Oyadomari S, Novoa I, Zhang Y, Jungreis R, Nagata K, et al. CHOP induces death by promoting protein synthesis and oxidation in the stressed endoplasmic reticulum. Genes Dev 2004;18:3066-3077.

26. Szegezdi E, Logue SE, Gorman AM, Samali A. Mediators of endoplasmic reticulum stress-induced apoptosis. EMBO Rep 2006;7:880-885.

27. Liang Y, Zheng T, Song R, Wang J, Yin D, Wang L, Liu H, et al. Hypoxia-mediated sorafenib resistance can be overcome by EF24 through Von Hippel-Lindau tumor suppressor-dependent HIF-1alpha inhibition in hepatocellular carcinoma. Hepatology 2013;57:1847-1857.

28. Peng S, Wang Y, Peng H, Chen D, Shen S, Peng B, Chen M, et al. Autocrine vascular endothelial growth factor signaling promotes cell proliferation and modulates sorafenib treatment efficacy in hepatocellular carcinoma. Hepatology 2014;60:1264-1277.

Figure legends

Fig. 1. Sorafenib induces ER stress in HCC cells. (A) Immunoblot of phospho-eIF2a from SNU761 cells that were treated with the indicated concentration of sorafenib for 24 hours. (B) CHOP mRNA expression in SNU761 cells was analyzed by RT-PCR. Thapsigargin, an ER stress inducer, was used as a positive control and GAPDH was used as a loading control. (C) Immunoblot of phospho-eIF2a from Huh7 cells that were treated with the indicated concentration of sorafenib for 24 hours. (D) *Left,* CHOP mRNA expression in Huh7 cells were analyzed by RT-PCR. β-actin was used as a loading control; *right*, CHOP mRNA expression was quantified by real-time PCR.

Fig. 2. The effect of sorafenib on the gene expression change of molecules in ER stress network. qRT-PCR experiments on SNU761 cells were done twice in 2 μM sorafenib and two or four times in 4 μM sorafenib. *P*-values were obtained through paired t-test or Wilcoxon signed ranks test and descriptive statistics was calculated from 4 μM tests. (A) UPR signal transducers. (B) Molecules involved in apoptosis. (C) Molecules participating in ER protein folding and quality control. (D) Ubiquitin-proteasome system. (E) Molecules involved in retrotranslocation (*, $P < 0.05$).

Fig. 3. The logic diagram of ER stress network and the simulation of PDI or proteasome inhibition. (A) The logic diagram of ER stress network and its inhibitors. (B) The simulation results of the model based on logical approximation of ODEs (see Materials and Method for details) (a.u., arbitrary unit).

Figure 4. PACMA 31 enhances the sorafenib-induced cytotoxicity. HCC cells were

treated with 4 μM sorafenib alone, 0.4 μM PACMA 31 alone, or in combination for 24 hours. (A) Cell viability assay in Hep3B, SNU475, HepG2, SNU761, and Huh7 cells. Experiments were repeated in triplicates. (B) Apoptosis assay in Hep3B, SNU475, HepG2 and SNU761 cells. Results are presented by means ± SEM (error bars). (C) To analyze cell death, PI was added to cells at a final concentration of 1 μg/mL. Images were taken 6 hours after each treatment.

Figure 5. The comparison between sorafenib alone and combination treatment on the gene expression change of molecules in ER stress network of SNU761 cells. (A) UPR signal transducers. (B) Molecules involved in apoptosis. (C) Molecules participating in ER protein folding and quality control. (D) Glycoprotein processing. (E) Ubiquitin-proteasome system. (F) Molecules involved in retrotranslocation (*, $P < 0.05$).

Figure 6. The combination treatment with PACMA 31 suppressed the growth of Hep3B xenografts *in vivo*. Female nude mice with Hep3B cells were divided into four groups and treated as previously described. (A) The change of tumor volume. (B) Pictures of tumors resected from mice.

Figure 7. Survival analysis according to the PDI expression level. (A) Time to progression. (B) Overall survival.

Table 1. The response of HCC patients to sorafenib according to the PDI expression level.

		PDI expression level		Number
		Low (Grade 0-1)	High (Grade 2-3)	
Clinical response	CR+PR+SD	8	3	11
	No response	28	56	84
	Response rate	22.2%	5.1%	95
p-value		0.018 (Fisher's exact test)		

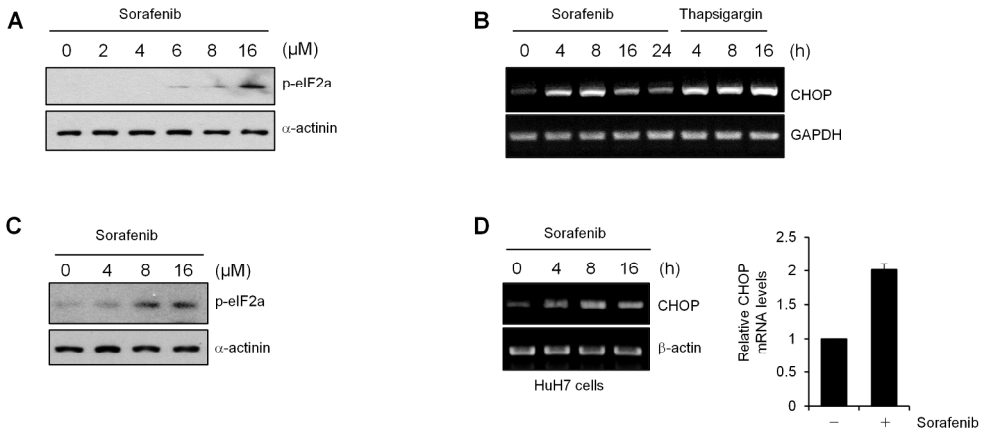

Figure 1

241x107mm (300 x 300 DPI)

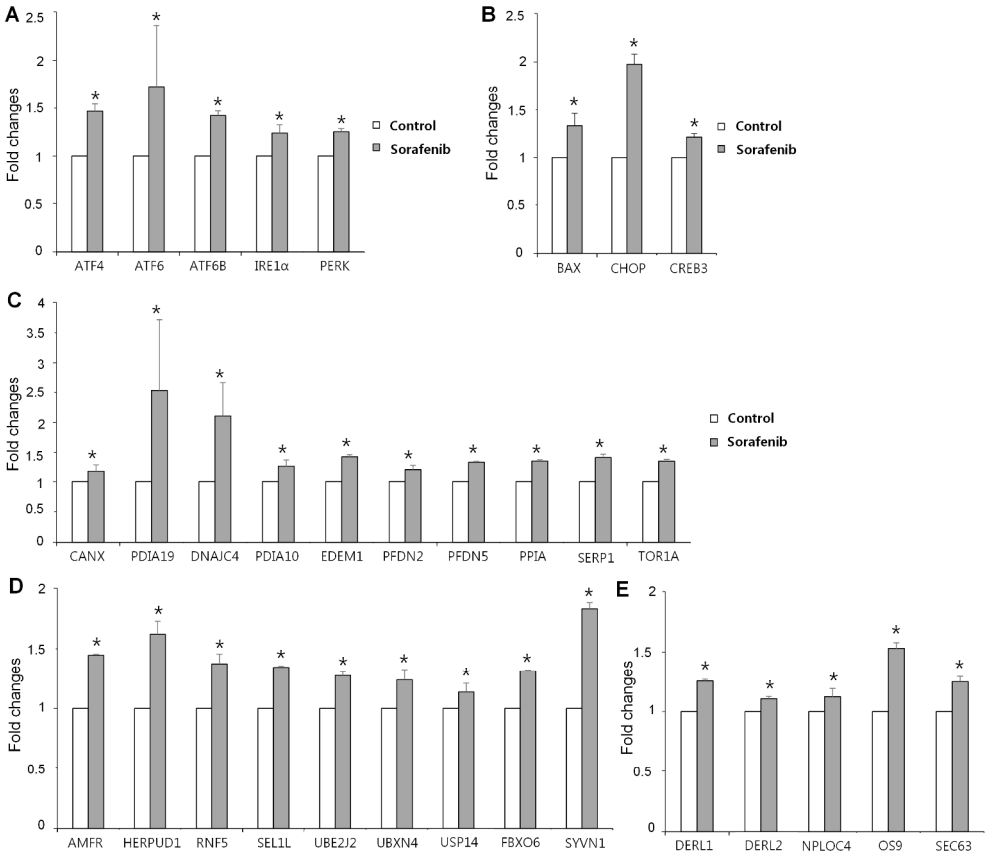

Figure 2

267x232mm (300 x 300 DPI)

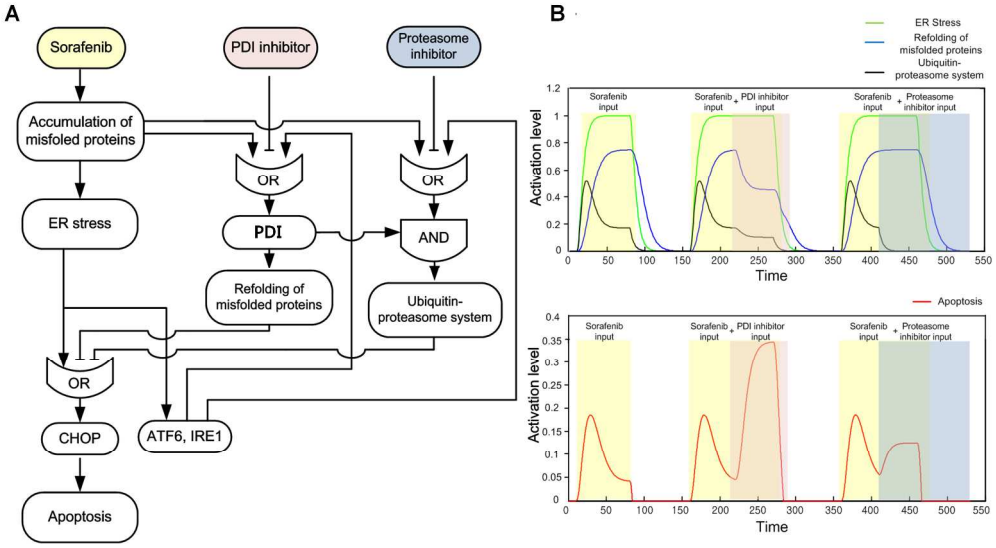

Figure 3

254x140mm (300 x 300 DPI)

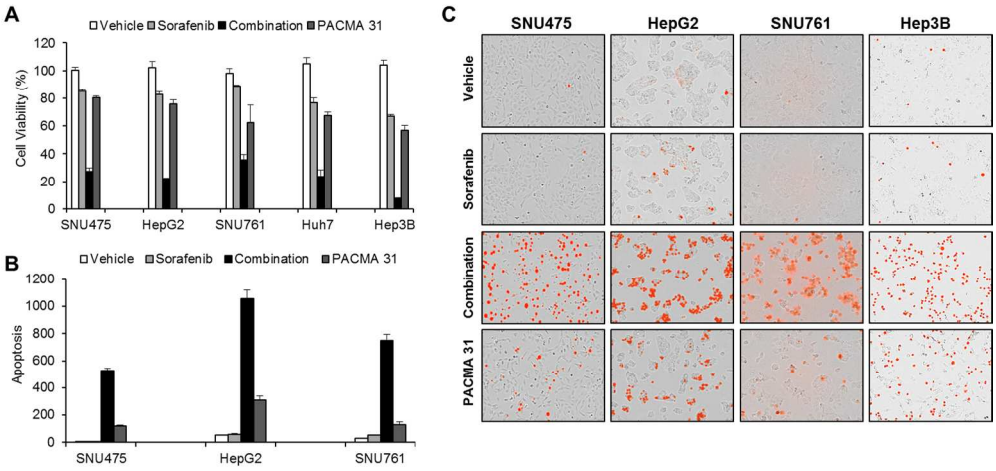

Figure 4

264x124mm (150 x 150 DPI)

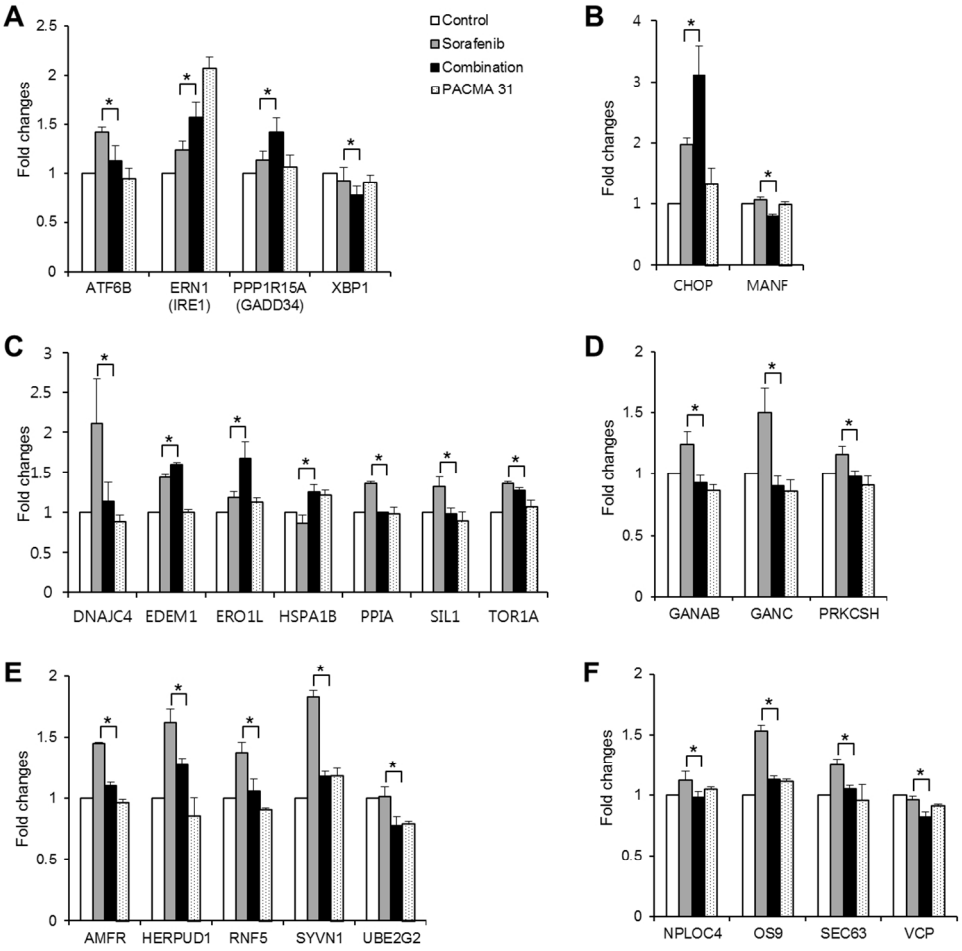

Figure 5

218x211mm (150 x 150 DPI)

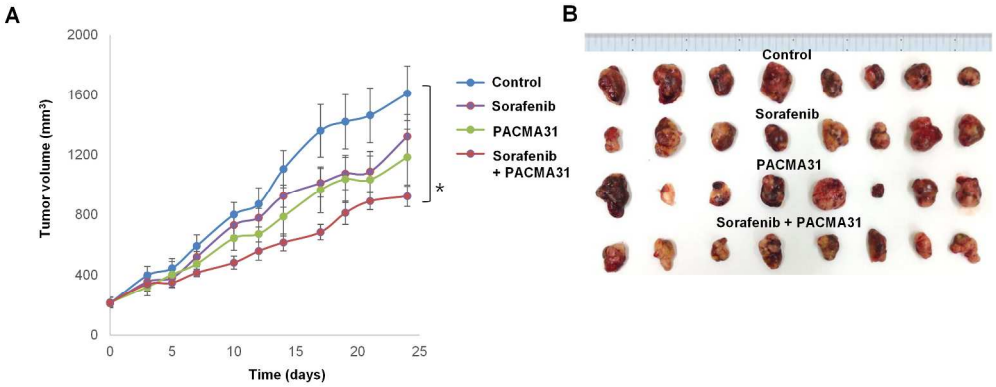

Figure 6

252x100mm (300 x 300 DPI)

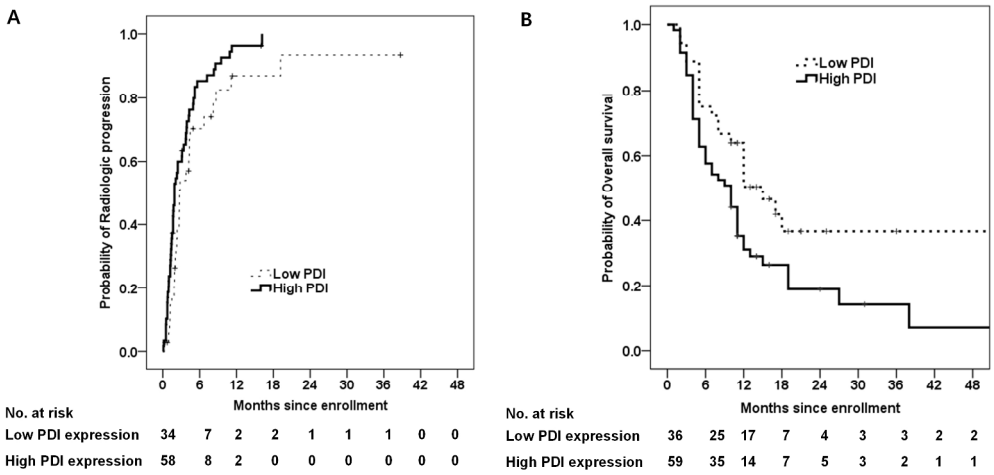

Figure 7

247x118mm (300 x 300 DPI)

Supporting information

Protein disulfide isomerase inhibition synergistically enhances the efficacy of sorafenib for hepatocellular carcinoma

Jae-Kyung Won, Su Jong Yu, Chae Young Hwang, Sung-Hwan Cho, Sang-Min Park, Kwangsoo Kim, Won-Mook Choi, Hyeki Cho, Eun Ju Cho, Jeong-Hoon Lee, Kyung Bun Lee, Yoon Jun Kim, Kyung-Suk Suh, Ja-June Jang, Chung Yong Kim, Jung-Hwan Yoon, Kwang-Hyun Cho*

Table of Contents

1. **Supporting Materials and Methods……...2**
2. **Supporting Tables……4**
3. **Supporting Figure Legends……11**
4. **References……..14**

Supporting Materials and Methods

mRNA microarray experiments and analysis

Total RNA was extracted using Trizol (Invitrogen Life Technologies, Carlsbad, CA), purified using RNeasy columns (Qiagen, Valencia, CA) according to the manufacturers' protocol. Total RNA was amplified and purified using the Ambion Illumina RNA amplification kit (Ambion, Austin, TX) to yield biotinylated cRNA according to the manufacturer's instructions. 750 ng of labeled cRNA samples were hybridized to each human HT-12 expression v.4 bead array for 16-18 h at 58°C, according to the manufacturer's instructions (Illumina, Inc., San Diego, CA). Detection of array signal was carried out using Amersham fluorolink streptavidin-Cy3 (GE Healthcare Bio-Sciences, Little Chalfont, UK) following the bead array manual. Arrays were scanned with an Illumina bead array Reader confocal scanner according to the manufacturer's instructions.

Raw data were extracted using the software provided by the manufacturer (Illumina GenomeStudio v2011.1 (Gene Expression Module v1.9.0)). Array probes transformed by logarithm and normalized by quantile method. Statistical significance of the expression data was determined using Fold change and LPE (Local Pooled Error) test in which the null hypothesis was that no difference exists among 2 groups. False discovery rate (FDR) was controlled by adjusting *P*-value using Benjamini-Hochberg algorithm. Basically, differentially expressed genes were acquired using the criteria of adjusted *P*-value < 0.05 and absolute fold change ≥ 1.5, except SNU761. In case of SNU761, which was the first cell line that was tested, three experiments were performed on different days each, so no gene met the criteria of

P-value. In this case, only the criteria of fold change ≥1.7 was applied to select candidate genes.

Gene list functional enrichment analysis and Gene-Set Enrichment Analysis (GSEA) using hallmark gene sets in MSigDB were performed using ToppGene Suite (https://toppgene.cchmc.org/) (1) and GSEA software (2), respectively. Data analysis and visualization of differentially expressed genes was also conducted using R 3.1.2 (www.r-project.org).

Supporting Tables

Table S1. 84 key molecules in qRT-PCR experiments and their changes resulting from sorafenib treatment in SNU761 cells.

Module	Gene lists	Differentially expressed genes (control vs sorafenib)	
		Upregulated in sorafenib treatment group ($P < 0.05$)	Downregulated in sorafenib treatment group ($P < 0.05$)
UPR signal transducer	ATF4, ATF6, ATF6B, ERN1 (IRE1a), ERN2 (IRE1b), EIF2A, EIF2AK3 (PERK), XBP1, PPP1R15A (GADD34)	ATF4, ATF6, ATF6B, ERN1 (IRE1a), EIF2AK3 (PERK)	None
Apoptosis	BAX, MANF, DDIT3 (CHOP), HTRA2, HTRA4, CEBPB, CREB3, CREB3L3, MAPK10, MAPK8, MAPK9	BAX, DDIT3 (CHOP), CREB3	None
ER protein folding and quality control	CALR, CANX, CCT4, CCT7, DNAJB2, DNAJB9, DNAJC10, DNAJC3, DNAJC4, EDEM1, EDEM3, ERO1L, ERO1LB, ERP44 (PDIA10), HSPA1B, HSPA1L, HSPA2, HSPA4, HSPA4L, HSPA5, HSPH1, NUCB1, PDIA3, PFDN2, PFDN5, PPIA, RPN1, SERP1, SIL1, TCP1, TOR1A	CANX, DNAJC10, DNAJC4, ERP44 (PDIA10), EDEM1, PFDN2, PFDN5, PPIA, SERP1, TOR1A	None
Glycoprotein processing	GANAB, GANC, PRKCSH, UGGT1, UGGT2	GANAB, UGGT1	None
Retrotranslocation	DERL1, DERL2, NPLOC4, OS9, SEC63, SELS	DERL1, DERL2, NPLOC4, OS9, SEC63	None
Ubiquitination	AMFR, ATXN3, FBXO6, HERPUD1, RNF139, RNF5, SEC62, SEL1L, SYVN1, UBE2G2, UBE2J2, UBXN4, UFD1L, USP14, VCP	AMFR, FBXO6, HERPUD1, RNF5, SEL1L, SYVN1, UBE2J2, UBXN4, USP14	None
Regulation of cholesterol metabolism	INSIG1, INSIG2, MBTPS1, MBTPS2, SCAP, SREBF1, SREBF2	INSIG1, INSIG2, SREBF2	None

Table S2. Baseline characteristics of study population.

Variable	Total (*n*=95)
Age (years) (median (range))	53 (20–76)
< 60	66 (69.5%)
≥ 60	29 (30.5%)
Gender	
Male	80 (84.2%)
Female	15 (15.8%)
Etiology	
HBsAg positive	78 (82.1%)
Anti-HCV positive	5 (5.3%)
Alcohol	2 (2.1%)
Unknown	10 (10.5%)
Child-Pugh score (median (range))	5 (5–8)
Alpha-fetoprotein (ng/mL)	
< 200	20 (21.1%)
≥ 200	75 (78.9%)
Tumor size	
< 5 cm	89 (93.7%)
≥ 5 cm	6 (6.3%)
Tumor number	2.84 ± 3.57
Vascular invasion	
No	86 (90.5%)
Yes	9 (9.5%)
Edmondson grade (worst)	

Grade 2	12 (12.6%)
Grade 3	32 (33.7%)
Grade 4	51 (53.7%)
PDI expression	
Low	36 (37.9%)
High	59 (62.1%)

PD, progressive disease; HBsAg, hepatitis B surface antigen; Anti-HCV, antibody against hepatitis C virus; PDI, protein disulfide isomerase.

Table S3. Factors identified on univariate and multivariate analyses that affect time to progression in HCC patients treated with sorafenib

Variable	Univariate Analysis		Multivariate Analysis	
	HR	*P* Value*	Adjusted HR	*P* Value*
Age (≥ 60 years)	0.505 (0.311–0.821)	0.006	0.558 (0.339–0.918)	0.022
Male	1.342 (0.752–2.394)	0.320		
Etiology				
anti-HCV positive versus HBsAg positive	0.789 (0.317–1.962)	0.610		
Alcohol versus HBsAg positive	1.656 (0.402–6.833)	0.485		
Unknown versus HBsAg positive	0.357 (0.153–0.833)	0.017		
Child-Pugh score	1.190 (0.861–1.644)	0.293		
AFP (ng/mL)				
≥ 200	1.275 (0.826–1.969)	0.273		
Tumor size				
≥ 5 cm	1.160 (0.468–2.878)	0.748		

Tumor number	1.025 (0.966–1.089)	0.419		
Vascular invasion				
Yes	0.648 (0.279–1.503)	0.312		
Lymph node				
Yes	2.229 (1.296–3.832)	0.004	2.368 (1.335–4.200)	0.003
Metastasis				
Yes	2.515 (1.153–5.484)	0.020	3.478 (1.559–7.761)	0.002
Edmondson grade (worst)				
Grade 3 versus grade 2	0.722 (0.347–1.505)	0.385		
Grade 4 versus grade 2	1.459 (0.709–3.005)	0.305		
PDI expression level				
High	1.629 (1.027–2.582)	0.038	1.833 (1.143–2.937)	0.012

Abbreviations: Anti-HCV, antibody against hepatitis C virus; HBsAg, hepatitis B surface antigen; AFP, alpha-fetoprotein; PDI, protein disulfide isomerase.

Table S4. Factors identified on univariate and multivariate analyses that affect overall survival in HCC patients treated with sorafenib

Variable	Univariate Analysis		Multivariate Analysis	
	HR	*P* Value*	Adjusted HR	*P* Value*
Age (≥ 60 years)	0.821 (0.482–1.398)	0.468		
Male	0.651 (0.310–1.364)	0.255		
Etiology				
anti-HCV positive versus HBsAg positive	2.048 (0.817–5.135)	0.126		
Alcohol versus HBsAg positive	0.765 (0.148–3.954)	0.749		
Unknown versus HBsAg positive	1.089 (0.126–9.393)	0.938		
Child-Pugh score	2.115 (1.469–3.044)	<0.001	1.966 (1.349–2.864)	<0.001
AFP (ng/mL)				
≥ 200	1.157 (0.716–1.870)	0.551		
Tumor size				
≥ 5 cm	1.386 (0.545–3.522)	0.493		

Tumor number	1.114 (1.046–1.186)	0.001	1.109 (1.037–1.186)	0.003
Vascular invasion				
Yes	1.599 (0.725–3.526)	0.244		
Lymph node				
Yes	2.749 (1.507–5.015)	0.001	2.135 (1.148–3.971)	0.017
Metastasis				
Yes	1.365 (0.622–2.996)	0.438		
Edmondson grade (worst)				
Grade 3 versus grade 2	1.334 (0.494–3.602)	0.569		
Grade 4 versus grade 2	3.576 (1.384–9.240)	0.009		
PDI expression level				
High	1.767 (1.051–2.971)	0.032	1.878 (1.107–3.184)	0.019

Abbreviations: Anti-HCV, antibody against hepatitis C virus; HBsAg, hepatitis B surface antigen; AFP, alpha-fetoprotein; PDI, protein disulfide isomerase.

Supporting Figures

Figure S1. HepG2, Hep3B, Huh7, SNU475, and SNU761 cells were treated with the indicated concentrations of sorafenib for 48 hours.

Figure S2. Cell viability assays of Hep3B cells expressing scrambled shRNA or CHOP shRNA. Scrambled and CHOP knockdown cells were treated with the indicated concentrations of sorafenib for 48 h. Knockdown of CHOP was confirmed by RT-PCR (insets). GAPDH was used as a loading control.

Figure S3. ER pathway network with upregulated molecules upon sorafenib treatment in SNU761 cells. Brown colored rectangles indicate the upregulated molecules or modules after sorafenib treatment.

Figure S4. The effect of sorafenib on the expression changes of molecules in ER stress network of HepG2 cell lines. qRT-PCR experiments were done in triplicate with 4 μM sorafenib. *P*-values were obtained through paired t-test. (A) UPR signal transducers. (B) Molecules involved in apoptosis. (C) Molecules participating in ER protein folding and quality control. (D) Ubiquitin-proteasome system. (E) Molecules involved in retrotranslocation (*, $P < 0.05$).

Figure S5. The effect of sorafenib on the expression change of molecules in ER stress network of Huh7. qRT-PCR experiments were done with 4 μM sorafenib. (A) UPR signal transducers. (B) Molecules involved in apoptosis. (C) Molecules participating in ER protein folding and quality control. (D) Glycoprotein processing.

(E) Ubiquitin-proteasome system. (F) Molecules involved in the regulation of cholesterol metabolism.

Figure S6. Reduction of ER stress network by the kernel identification algorithm. Red and blue links denote positive and negative regulations, respectively. (A) Original ER stress network. (B) Reduced network identified by the kernel network analysis.

Figure S7. Simulations according to the different coefficient values. (A) w_9=0.9, w_{10}=0.2. (B) w_9=0.6, w_{10}=0.8.

Figure S8. Bortezomib does not induce the synergistic cytotoxicity with sorafenib in SNU761 cells. (A) SNU761 cells were treated with 4 μM sorafenib alone, 0.1 μM Bortezomib alone, or in combination for 24 hours. (B) SNU761 cells were treated with 4 μM sorafenib alone, 0.2 μM Bortezomib alone, or in combination for 24 hours. Cell viability was determined using WST-1 solution. Experiments were repeated in triplicates.

Figure S9. ER stress network with the expression change of molecules upon sorafenib alone or PACMA 31 combination treatment in SNU761 cells. Brown, green and blue colored rectangles denote the upregulated or down-regulated molecules after each treatment as indicated in the right upper side legends.

Figure S10. The comparison between sorafenib alone and combination treatment on the gene expression change of molecules in ER stress network of HepG2 cells. (A)

UPR signal transducers. (B) Molecules involved in apoptosis. (C) Molecules participating in ER protein folding and quality control. (D) The regulation of cholesterol metabolism. (E) Ubiquitin-proteasome system. (F) Molecules involved in retrotranslocation (*, $P < 0.05$).

Figure S11. Cell viability assays of (A) HepG2 and (B) SNU475 cells expressing control vector or a PDI expression plasmid. Ectopic overexpression of PDI was confirmed by immunoblotting (insets). GAPDH was used as a loading control.

References

1. Chen J, Bardes EE, Aronow BJ, Jegga AG. ToppGene Suite for gene list enrichment analysis and candidate gene prioritization. Nucleic Acids Res 2009;37:W305-311.

2. Subramanian A, Tamayo P, Mootha VK, Mukherjee S, Ebert BL, Gillette MA, Paulovich A, et al. Gene set enrichment analysis: a knowledge-based approach for interpreting genome-wide expression profiles. Proc Natl Acad Sci U S A 2005;102:15545-15550.

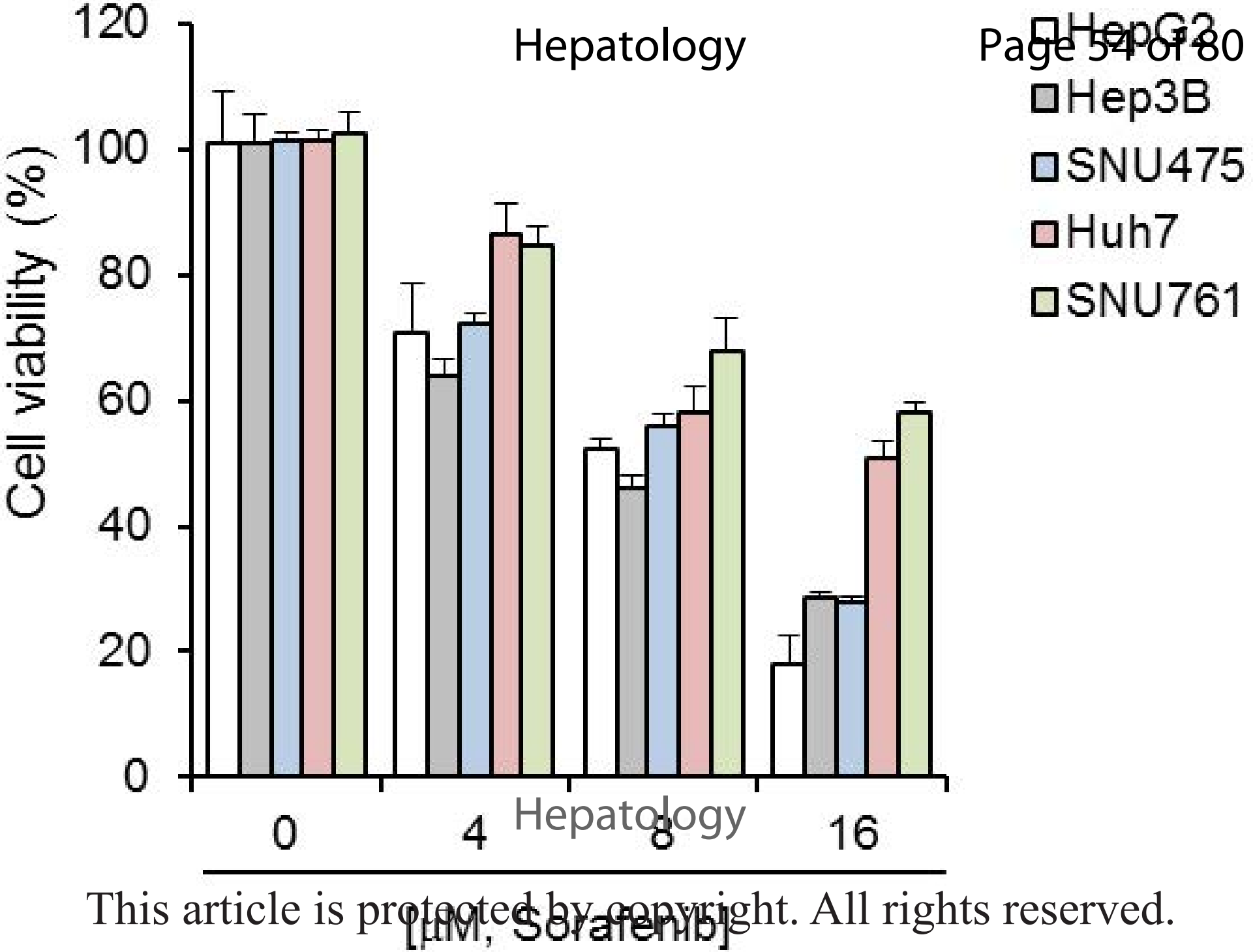

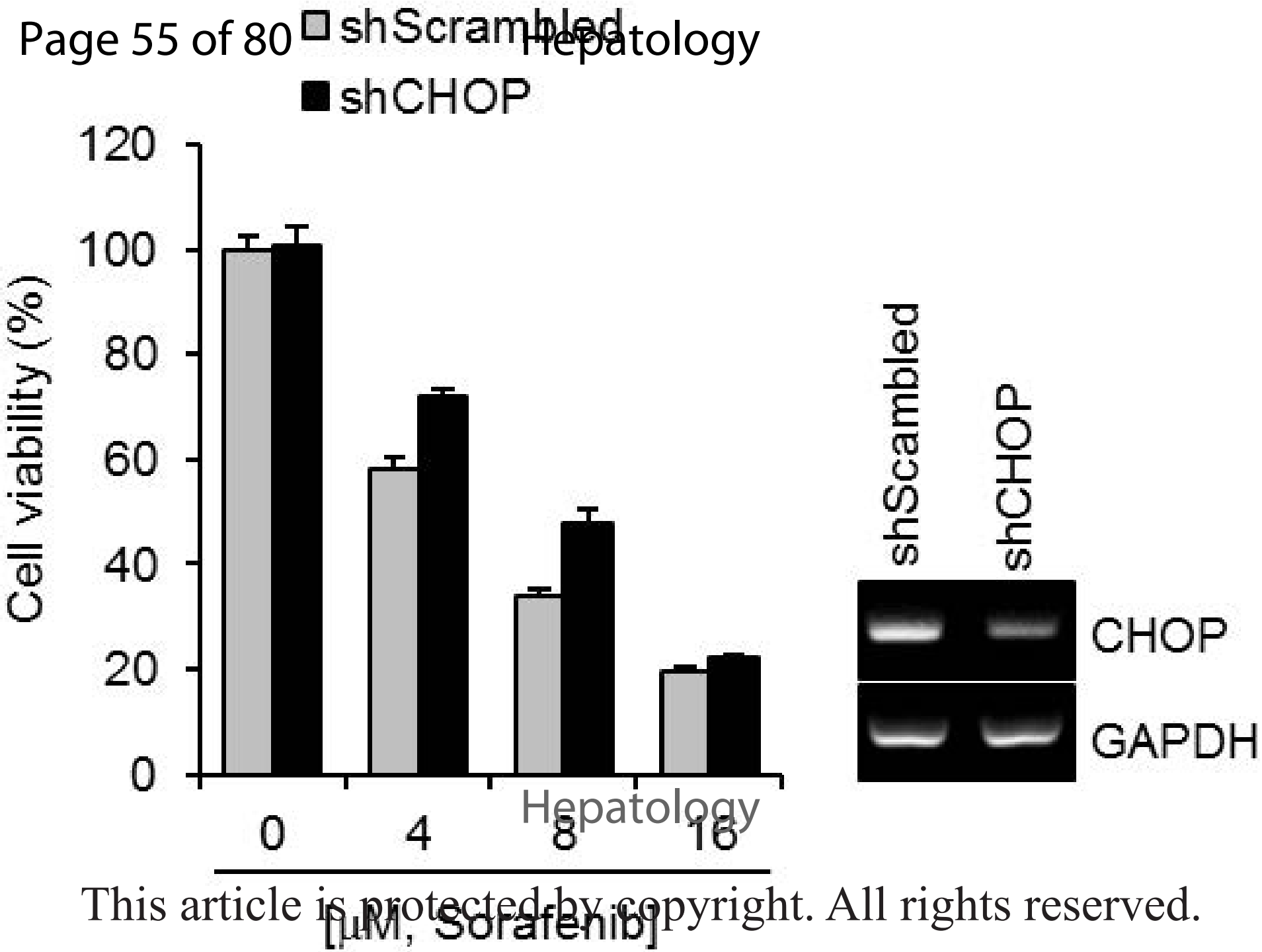

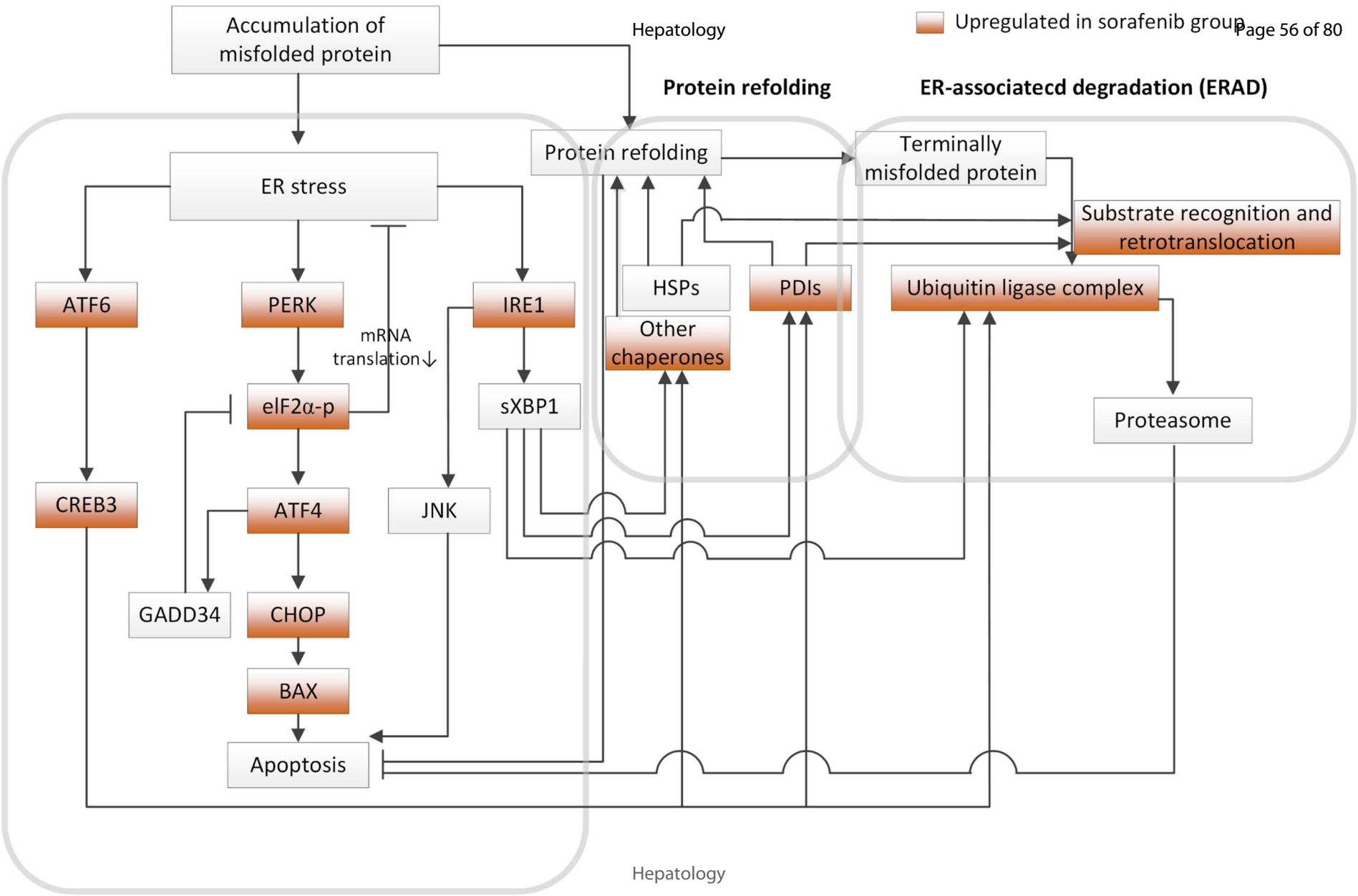

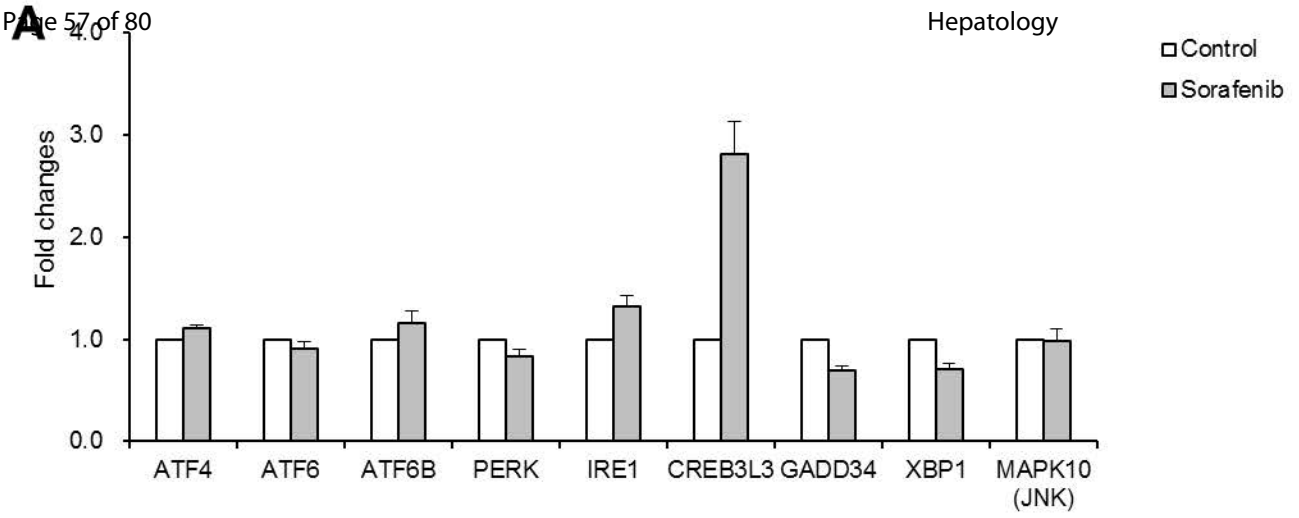

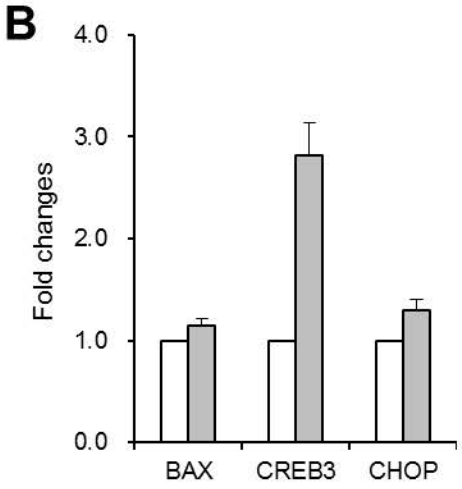

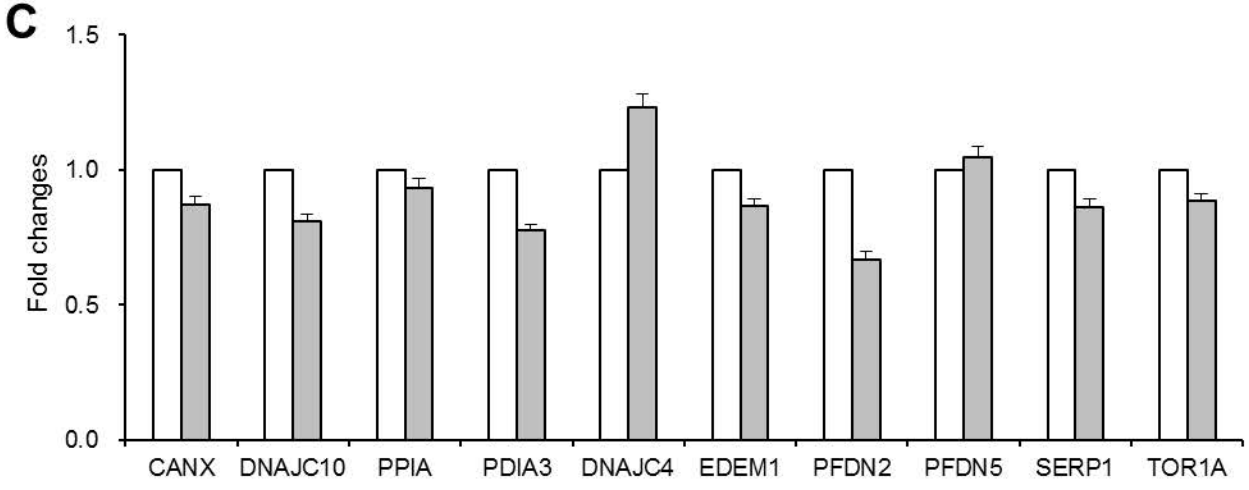

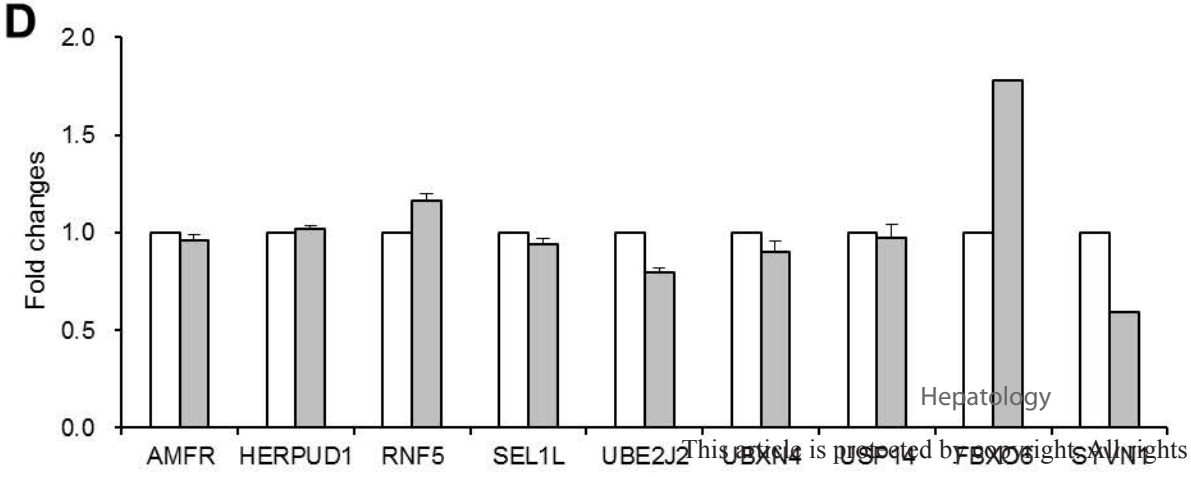

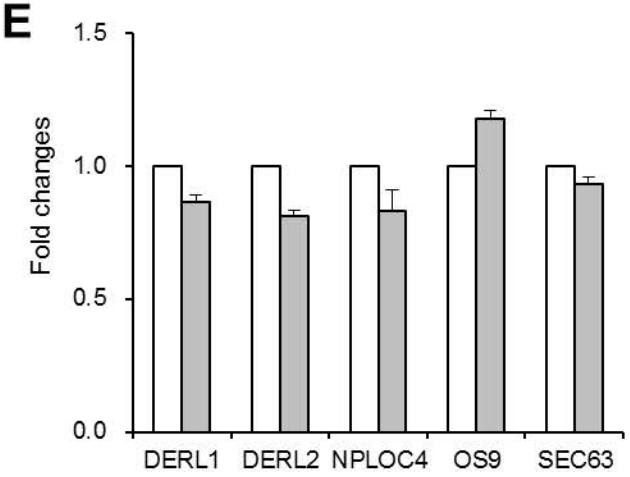

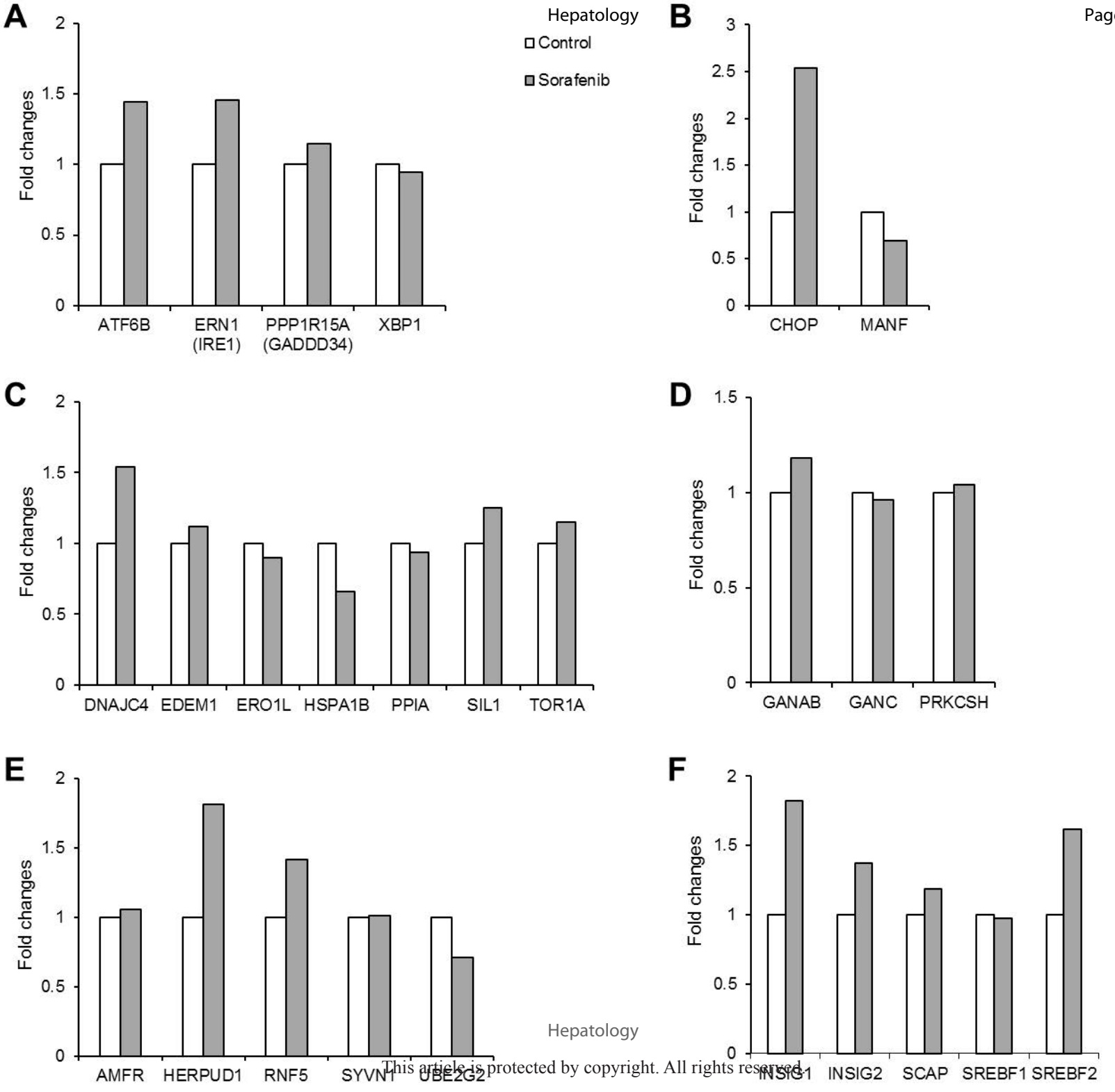

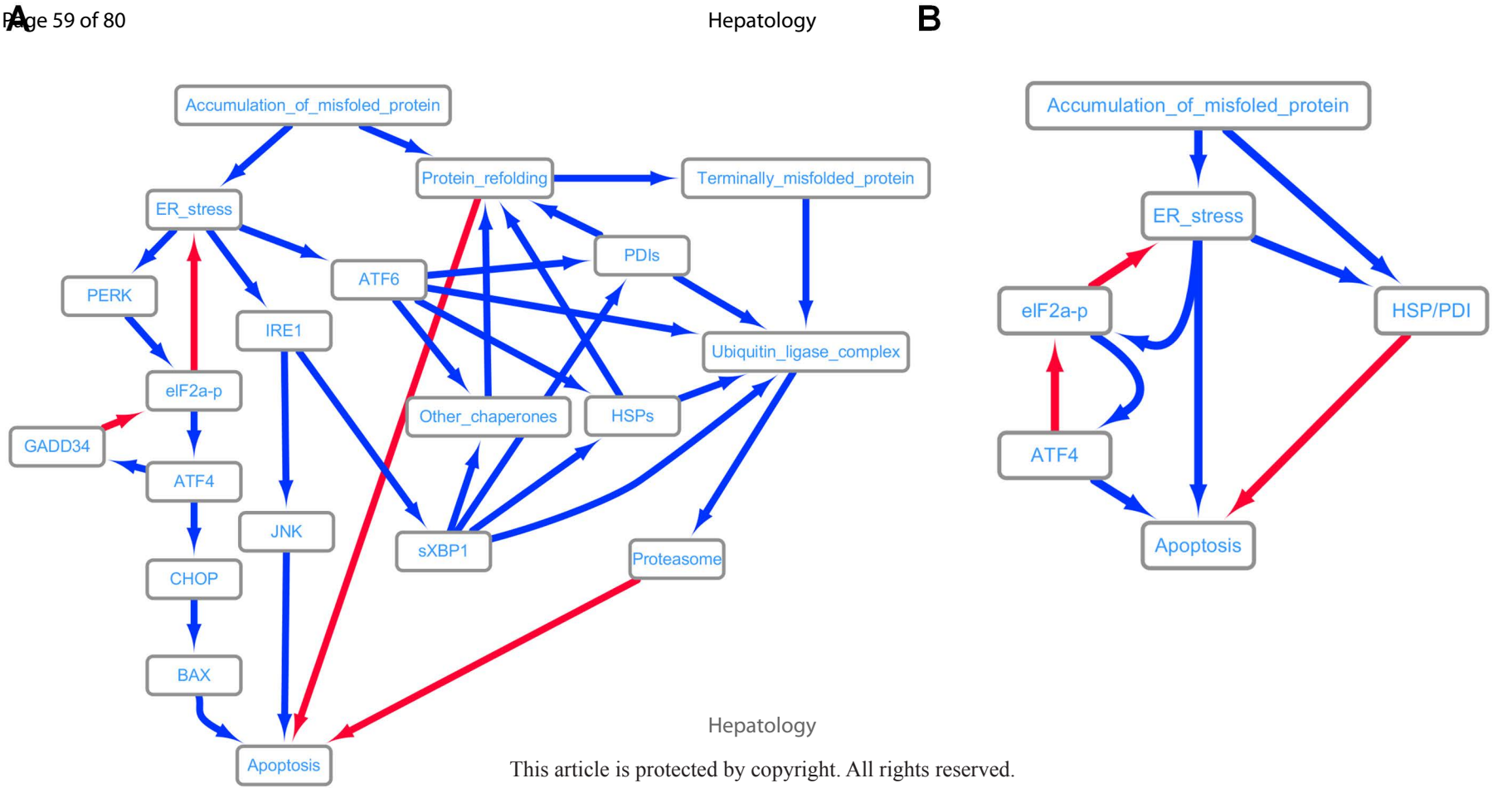

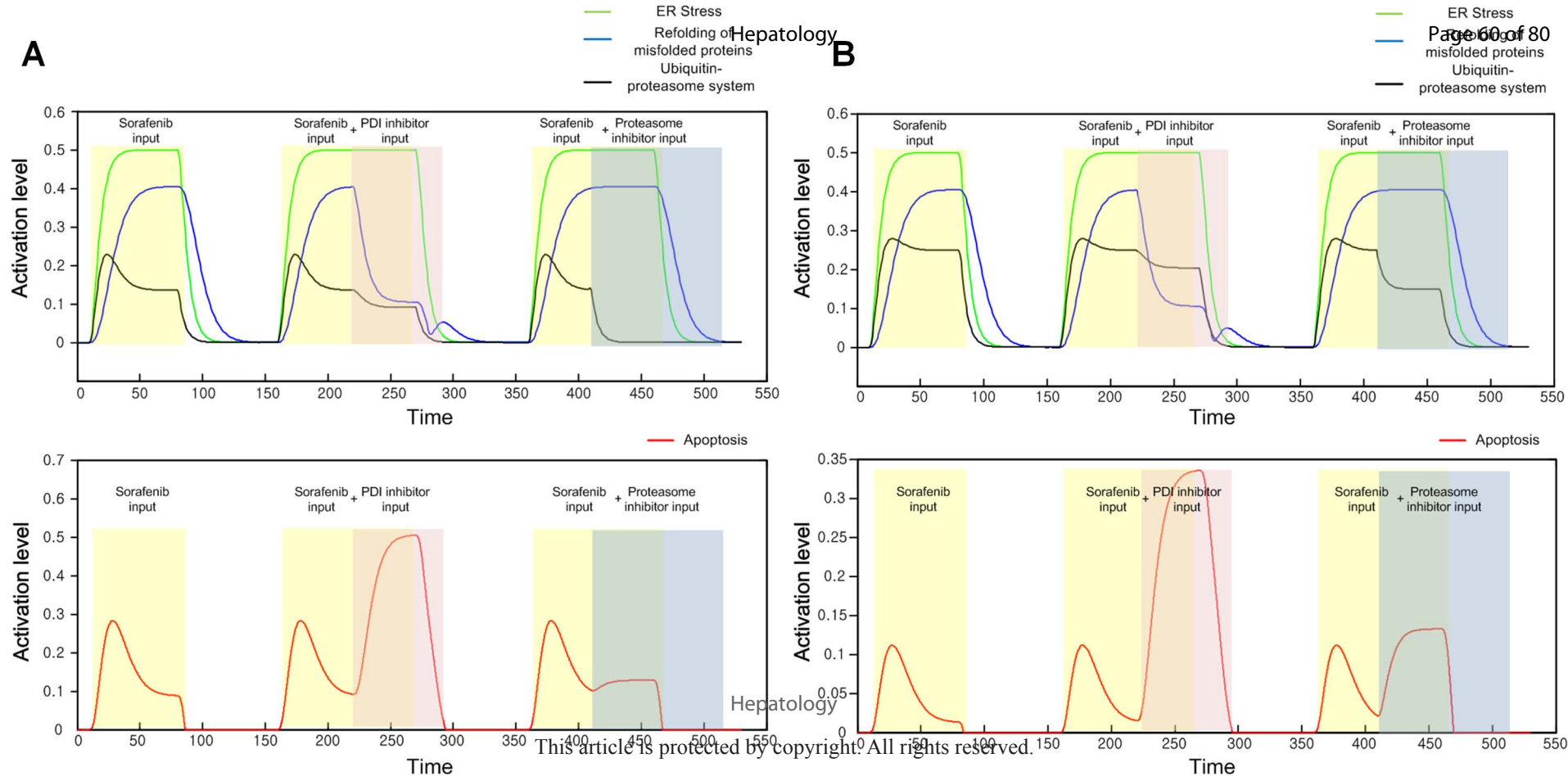

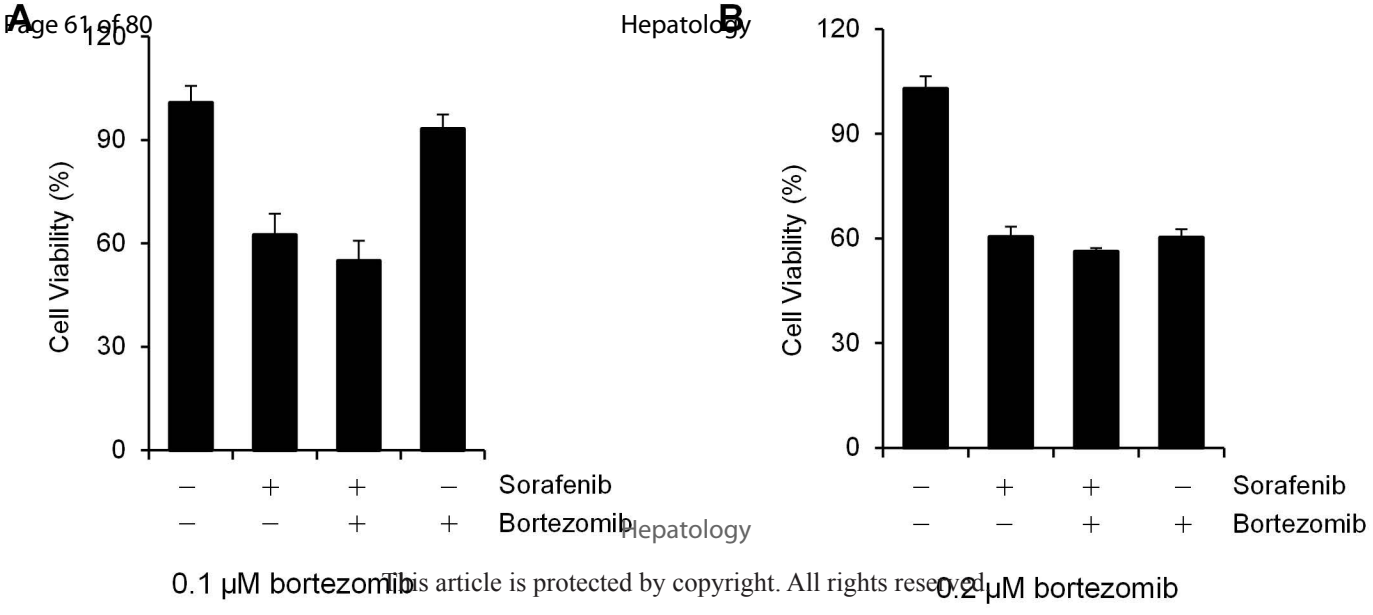

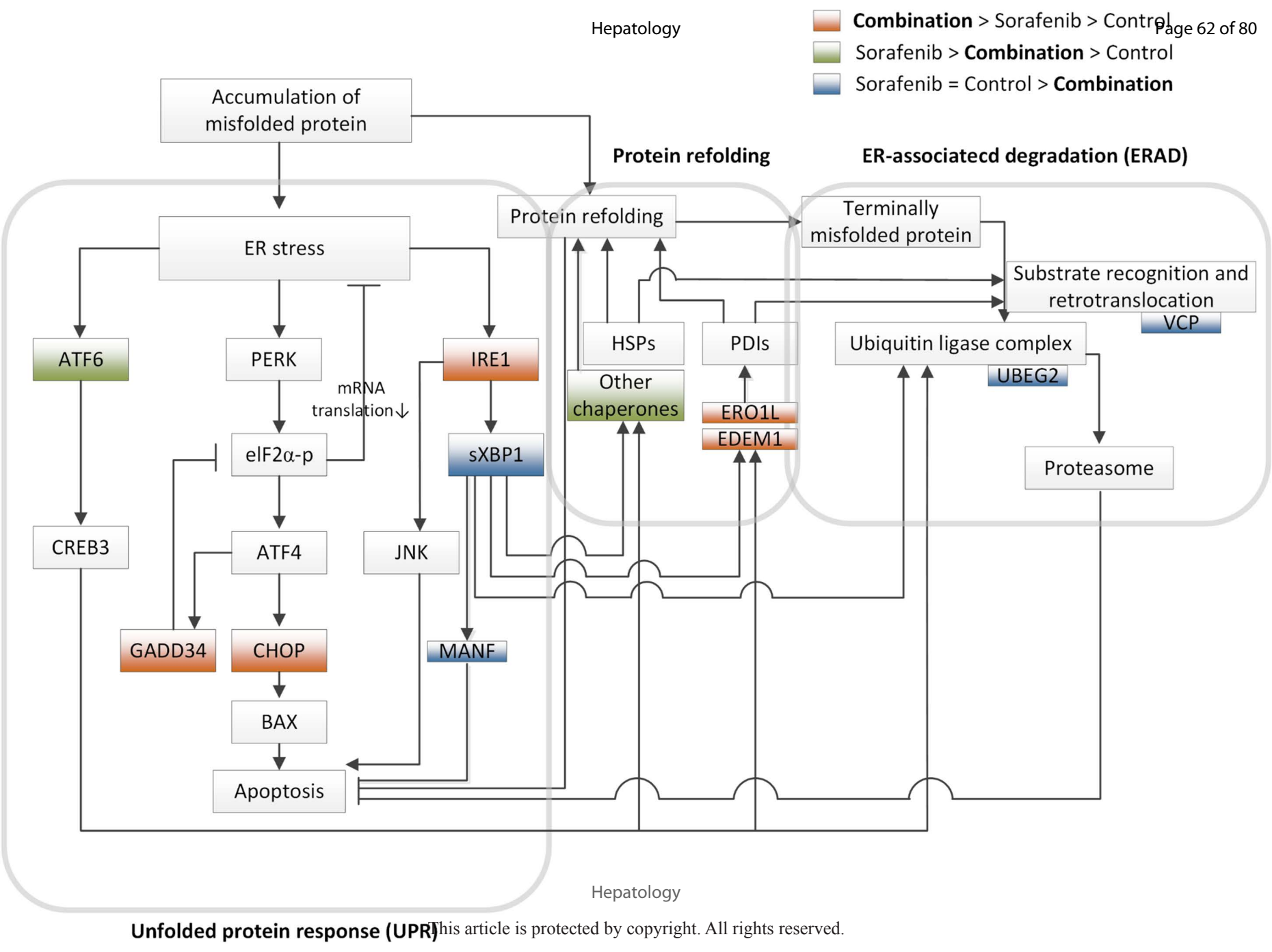

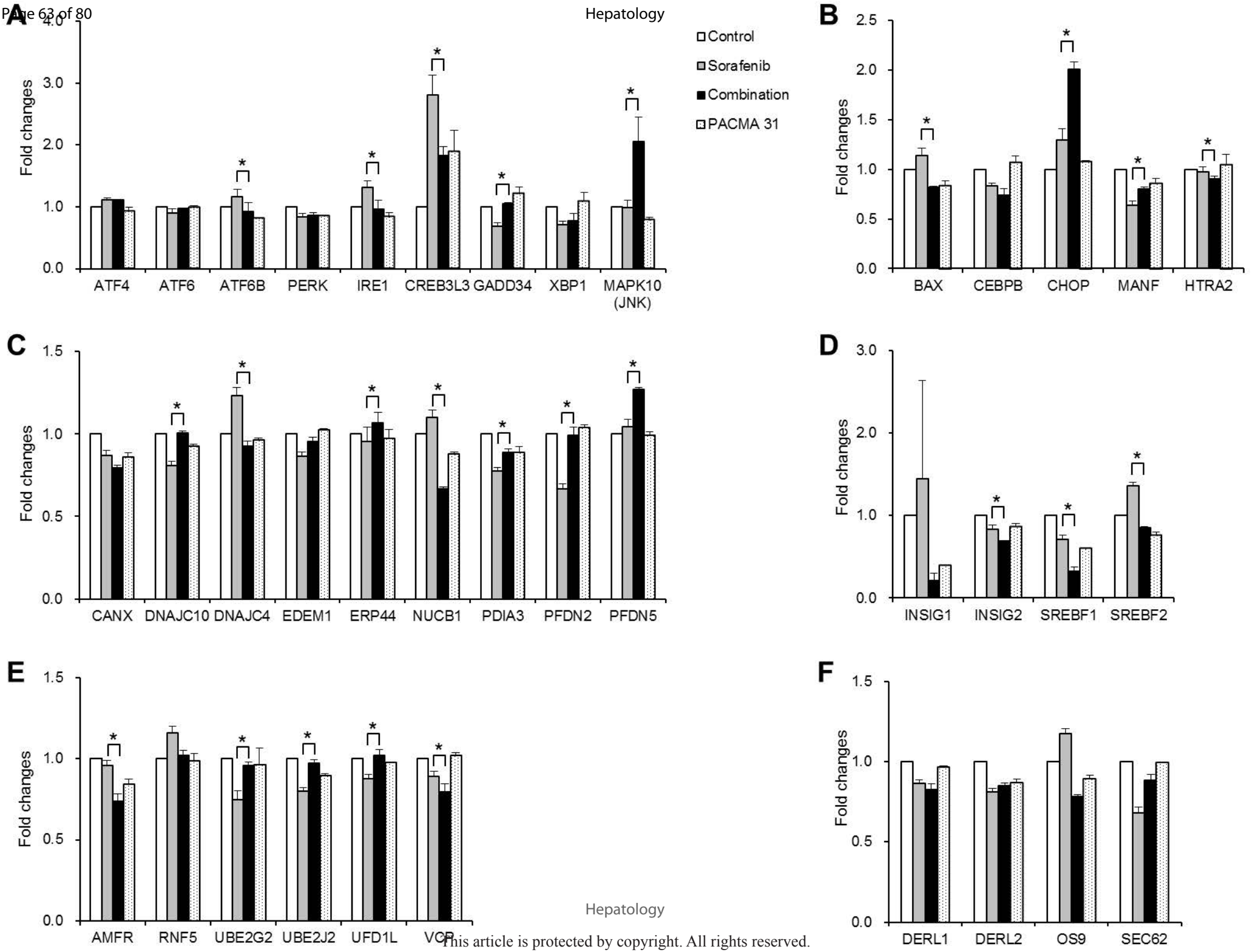

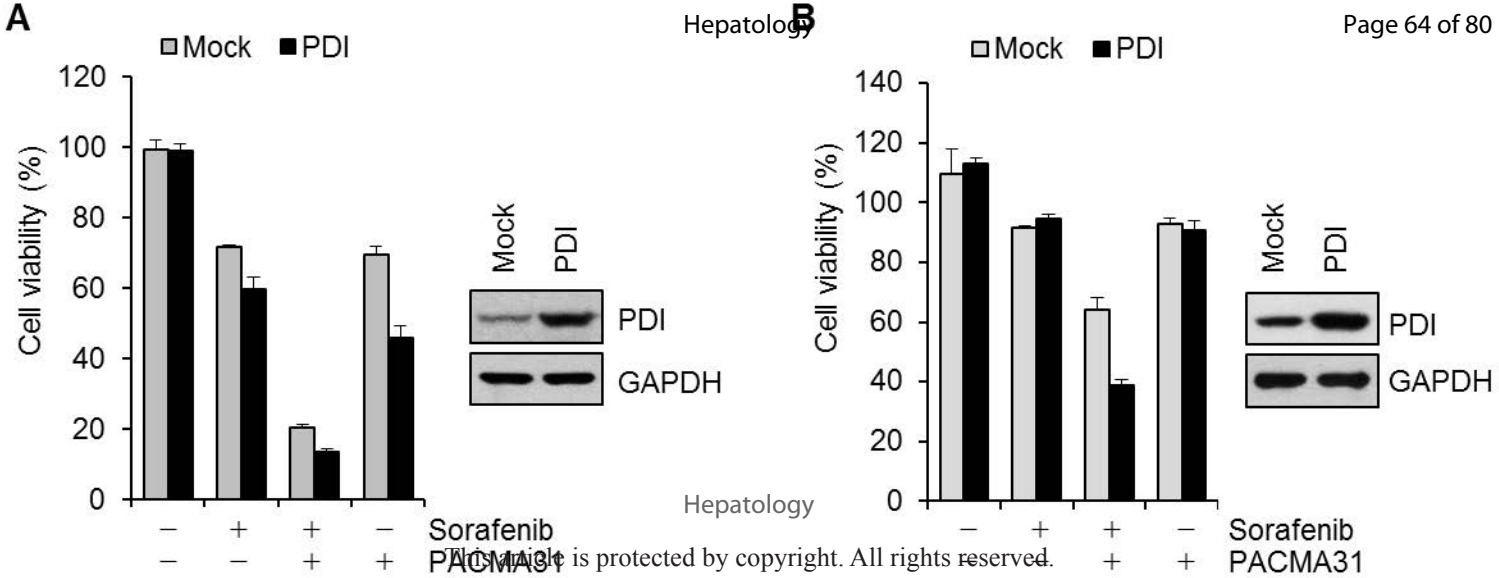

SNU761					
Category	ID	Name	Source	p-value	q-value FDR B&H
Coexpression	M5890	Genes regulated by NF-kB in response to TNF [GeneID=7124].	MSigDB H: Hallmark Gene Sets (v5.1)	1.13E-14	8.10E-12
Coexpression	M5891	Genes up-regulated in response to low oxygen levels (hypoxia).	MSigDB H: Hallmark Gene Sets (v5.1)	3.32E-10	6.91E-08
Coexpression	M5902	Genes mediating programmed cell death (apoptosis) by activation of caspases.	MSigDB H: Hallmark Gene Sets (v5.1)	3.71E-07	2.30E-05
Coexpression	M5939	Genes involved in p53 pathways and networks.	MSigDB H: Hallmark Gene Sets (v5.1)	2.68E-06	1.21E-04
Coexpression	M5924	Genes up-regulated through activation of mTORC1 complex.	MSigDB H: Hallmark Gene Sets (v5.1)	1.32E-04	2.62E-03
Coexpression	M5947	Genes up-regulated by STAT5 in response to IL2 stimulation.	MSigDB H: Hallmark Gene Sets (v5.1)	7.72E-04	9.74E-03
Coexpression	M5945	Genes involved in metabolism of heme (a cofactor consisting of iron and porphyrin) and erythroblast differentiation.	MSigDB H: Hallmark Gene	7.72E-04	9.74E-03

			Sets (v5.1)		
Coexpression	M5930	Genes defining epithelial-mesenchymal transition, as in wound healing, fibrosis and metastasis.	MSigDB H: Hallmark Gene Sets (v5.1)	7.72E-04	9.74E-03
Coexpression	M5953	Genes up-regulated by KRAS activation.	MSigDB H: Hallmark Gene Sets (v5.1)	7.72E-04	9.74E-03
Coexpression	M5922	Genes up-regulated during unfolded protein response, a cellular stress response related to the endoplasmic reticulum.	MSigDB H: Hallmark Gene Sets (v5.1)	1.59E-03	1.84E-02
Coexpression	M5897	Genes up-regulated by IL6 [GeneID=3569] via STAT3 [GeneID=6774], e.g., during acute phase response.	MSigDB H: Hallmark Gene Sets (v5.1)	4.10E-03	3.24E-02

Huh7					
Category	ID	Name	Source	p-value	q-value FDR B&H
Coexpression	M5924	Genes up-regulated through activation of mTORC1 complex.	MSigDB H: Hallmark Gene Sets (v5.1)	2.71E-12	6.02E-09
Coexpression	M5891	Genes up-regulated in response to low oxygen levels (hypoxia).	MSigDB H: Hallmark Gene	3.38E-11	5.06E-08

			Sets (v5.1)		
Coexpression	M5937	Genes encoding proteins involved in glycolysis and gluconeogenesis.	MSigDB H: Hallmark Gene Sets (v5.1)	3.67E-07	7.07E-05
Coexpression	M5922	Genes up-regulated during unfolded protein response, a cellular stress response related to the endoplasmic reticulum.	MSigDB H: Hallmark Gene Sets (v5.1)	2.42E-05	1.72E-03
Coexpression	M5942	Genes down-regulated in response to ultraviolet (UV) radiation.	MSigDB H: Hallmark Gene Sets (v5.1)	1.13E-04	5.23E-03
Coexpression	M5906	Genes defining early response to estrogen.	MSigDB H: Hallmark Gene Sets (v5.1)	1.43E-04	5.23E-03
Coexpression	M5932	Genes defining inflammatory response.	MSigDB H: Hallmark Gene Sets (v5.1)	8.29E-04	1.62E-02
Coexpression	M5941	Genes up-regulated in response to ultraviolet (UV) radiation.	MSigDB H: Hallmark Gene Sets (v5.1)	1.29E-03	2.35E-02
Coexpression	M5902	Genes mediating programmed cell death (apoptosis) by activation of caspases.	MSigDB H: Hallmark Gene Sets (v5.1)	1.42E-03	2.54E-02
Coexpression	M5925	Genes encoding cell cycle related targets of E2F transcription factors.	MSigDB H:	4.18E-03	4.23E-02

			Hallmark Gene Sets (v5.1)		
Coexpression	M5890	Genes regulated by NF-kB in response to TNF [GeneID=7124].	MSigDB H: Hallmark Gene Sets (v5.1)	4.18E-03	4.23E-02
Coexpression	M5907	Genes defining late response to estrogen.	MSigDB H: Hallmark Gene Sets (v5.1)	4.18E-03	4.23E-02
Coexpression	M5939	Genes involved in p53 pathways and networks.	MSigDB H: Hallmark Gene Sets (v5.1)	4.18E-03	4.23E-02

Hep3B					
Category	ID	Name	Source	p-value	q-value FDR B&H
Coexpression	M5892	Genes involved in cholesterol homeostasis.	MSigDB H: Hallmark Gene Sets (v5.1)	6.72E-19	3.33E-16
Coexpression	M5924	Genes up-regulated through activation of mTORC1 complex.	MSigDB H: Hallmark Gene Sets (v5.1)	1.11E-15	2.84E-13
Coexpression	M5890	Genes regulated by NF-kB in response to TNF [GeneID=7124].	MSigDB H:	1.80E-12	2.16E-10

			Hallmark Gene Sets (v5.1)		
Coexpression	M5908	Genes defining response to androgens.	MSigDB H: Hallmark Gene Sets (v5.1)	9.97E-10	5.95E-08
Coexpression	M5922	Genes up-regulated during unfolded protein response, a cellular stress response related to the endoplasmic reticulum.	MSigDB H: Hallmark Gene Sets (v5.1)	6.46E-09	3.03E-07
Coexpression	M5891	Genes up-regulated in response to low oxygen levels (hypoxia).	MSigDB H: Hallmark Gene Sets (v5.1)	7.30E-09	3.27E-07
Coexpression	M5939	Genes involved in p53 pathways and networks.	MSigDB H: Hallmark Gene Sets (v5.1)	7.30E-09	3.27E-07
Coexpression	M5925	Genes encoding cell cycle related targets of E2F transcription factors.	MSigDB H: Hallmark Gene Sets (v5.1)	6.14E-07	1.48E-05
Coexpression	M5901	Genes involved in the G2/M checkpoint, as in progression through the cell division cycle.	MSigDB H: Hallmark Gene Sets (v5.1)	2.43E-06	4.59E-05
Coexpression	M5902	Genes mediating programmed cell death (apoptosis) by activation of caspases.	MSigDB H: Hallmark Gene Sets (v5.1)	6.61E-06	1.10E-04

Coexpression	M5907	Genes defining late response to estrogen.	MSigDB H: Hallmark Gene Sets (v5.1)	9.10E-06	1.35E-04
Coexpression	M5937	Genes encoding proteins involved in glycolysis and gluconeogenesis.	MSigDB H: Hallmark Gene Sets (v5.1)	9.10E-06	1.35E-04
Coexpression	M5930	Genes defining epithelial-mesenchymal transition, as in wound healing, fibrosis and metastasis.	MSigDB H: Hallmark Gene Sets (v5.1)	9.10E-06	1.35E-04
Coexpression	M5934	Genes encoding proteins involved in processing of drugs and other xenobiotics.	MSigDB H: Hallmark Gene Sets (v5.1)	3.23E-05	3.90E-04
Coexpression	M5942	Genes down-regulated in response to ultraviolet (UV) radiation.	MSigDB H: Hallmark Gene Sets (v5.1)	1.05E-04	1.06E-03
Coexpression	M5905	Genes up-regulated during adipocyte differentiation (adipogenesis).	MSigDB H: Hallmark Gene Sets (v5.1)	1.08E-04	1.06E-03
Coexpression	M5893	Genes important for mitotic spindle assembly.	MSigDB H: Hallmark Gene Sets (v5.1)	1.08E-04	1.06E-03
Coexpression	M5896	Genes up-regulated in response to TGFB1 [GeneID=7040].	MSigDB H: Hallmark Gene	1.84E-04	1.74E-03

			Sets (v5.1)		
Coexpression	M5935	Genes encoding proteins involved in metabolism of fatty acids.	MSigDB H: Hallmark Gene Sets (v5.1)	2.79E-04	2.51E-03
Coexpression	M5941	Genes up-regulated in response to ultraviolet (UV) radiation.	MSigDB H: Hallmark Gene Sets (v5.1)	2.79E-04	2.51E-03
Coexpression	M5953	Genes up-regulated by KRAS activation.	MSigDB H: Hallmark Gene Sets (v5.1)	3.39E-04	2.67E-03
Coexpression	M5915	Genes encoding components of apical junction complex.	MSigDB H: Hallmark Gene Sets (v5.1)	3.39E-04	2.67E-03
Coexpression	M5946	Genes encoding components of blood coagulation system; also up-regulated in platelets.	MSigDB H: Hallmark Gene Sets (v5.1)	8.79E-04	6.19E-03
Coexpression	M5945	Genes involved in metabolism of heme (a cofactor consisting of iron and porphyrin) and erythroblast differentiation.	MSigDB H: Hallmark Gene Sets (v5.1)	2.76E-03	1.34E-02
Coexpression	M5906	Genes defining early response to estrogen.	MSigDB H: Hallmark Gene Sets (v5.1)	2.76E-03	1.34E-02
Coexpression	M5947	Genes up-regulated by STAT5 in response to IL2 stimulation.	MSigDB H:	2.76E-03	1.34E-02

			Hallmark Gene Sets (v5.1)		
Coexpression	M5949	Genes encoding components of peroxisome.	MSigDB H: Hallmark Gene Sets (v5.1)	3.88E-03	1.82E-02
Coexpression	M5897	Genes up-regulated by IL6 [GeneID=3569] via STAT3 [GeneID=6774], e.g., during acute phase response.	MSigDB H: Hallmark Gene Sets (v5.1)	4.38E-03	2.03E-02
Coexpression	M5913	Genes up-regulated in response to IFNG [GeneID=3458].	MSigDB H: Hallmark Gene Sets (v5.1)	7.11E-03	2.72E-02

HepG2					
Category	ID	Name	Source	p-value	q-value FDR B&H
Coexpression	M5891	Genes up-regulated in response to low oxygen levels (hypoxia).	MSigDB H: Hallmark Gene Sets (v5.1)	2.80E-13	1.47E-10
Coexpression	M5890	Genes regulated by NF-kB in response to TNF [GeneID=7124].	MSigDB H: Hallmark Gene Sets (v5.1)	2.80E-13	1.47E-10
Coexpression	M5934	Genes encoding proteins involved in processing of drugs and other	MSigDB H:	2.80E-13	1.47E-10

		xenobiotics.	Hallmark Gene Sets (v5.1)		
Coexpression	M5892	Genes involved in cholesterol homeostasis.	MSigDB H: Hallmark Gene Sets (v5.1)	1.18E-12	4.62E-10
Coexpression	M5953	Genes up-regulated by KRAS activation.	MSigDB H: Hallmark Gene Sets (v5.1)	5.94E-11	1.67E-08
Coexpression	M5946	Genes encoding components of blood coagulation system; also up-regulated in platelets.	MSigDB H: Hallmark Gene Sets (v5.1)	1.43E-09	2.19E-07
Coexpression	M5930	Genes defining epithelial-mesenchymal transition, as in wound healing, fibrosis and metastasis.	MSigDB H: Hallmark Gene Sets (v5.1)	1.69E-09	2.56E-07
Coexpression	M5924	Genes up-regulated through activation of mTORC1 complex.	MSigDB H: Hallmark Gene Sets (v5.1)	4.00E-08	3.17E-06
Coexpression	M5947	Genes up-regulated by STAT5 in response to IL2 stimulation.	MSigDB H: Hallmark Gene Sets (v5.1)	7.71E-07	3.76E-05
Coexpression	M5942	Genes down-regulated in response to ultraviolet (UV) radiation.	MSigDB H: Hallmark Gene Sets (v5.1)	2.47E-06	9.68E-05

Coexpression	M5928	A subgroup of genes regulated by MYC - version 2 (v2).	MSigDB H: Hallmark Gene Sets (v5.1)	3.79E-06	1.34E-04
Coexpression	M5921	Genes encoding components of the complement system, which is part of the innate immune system.	MSigDB H: Hallmark Gene Sets (v5.1)	1.20E-05	3.14E-04
Coexpression	M5905	Genes up-regulated during adipocyte differentiation (adipogenesis).	MSigDB H: Hallmark Gene Sets (v5.1)	1.20E-05	3.14E-04
Coexpression	M5948	Genes involve in metabolism of bile acids and salts.	MSigDB H: Hallmark Gene Sets (v5.1)	1.33E-05	3.42E-04
Coexpression	M5949	Genes encoding components of peroxisome.	MSigDB H: Hallmark Gene Sets (v5.1)	3.02E-05	6.98E-04
Coexpression	M5935	Genes encoding proteins involved in metabolism of fatty acids.	MSigDB H: Hallmark Gene Sets (v5.1)	3.38E-05	7.57E-04
Coexpression	M5907	Genes defining late response to estrogen.	MSigDB H: Hallmark Gene Sets (v5.1)	4.32E-05	8.58E-04
Coexpression	M5908	Genes defining response to androgens.	MSigDB H: Hallmark Gene	1.09E-04	1.88E-03

			Sets (v5.1)		
Coexpression	M5906	Genes defining early response to estrogen.	MSigDB H: Hallmark Gene Sets (v5.1)	1.47E-04	2.13E-03
Coexpression	M5939	Genes involved in p53 pathways and networks.	MSigDB H: Hallmark Gene Sets (v5.1)	1.47E-04	2.13E-03
Coexpression	M5937	Genes encoding proteins involved in glycolysis and gluconeogenesis.	MSigDB H: Hallmark Gene Sets (v5.1)	4.67E-04	4.93E-03
Coexpression	M5932	Genes defining inflammatory response.	MSigDB H: Hallmark Gene Sets (v5.1)	4.67E-04	4.93E-03
Coexpression	M5915	Genes encoding components of apical junction complex.	MSigDB H: Hallmark Gene Sets (v5.1)	4.67E-04	4.93E-03
Coexpression	M5909	Genes involved in development of skeletal muscle (myogenesis).	MSigDB H: Hallmark Gene Sets (v5.1)	4.67E-04	4.93E-03
Coexpression	M5922	Genes up-regulated during unfolded protein response, a cellular stress response related to the endoplasmic reticulum.	MSigDB H: Hallmark Gene Sets (v5.1)	1.17E-03	1.08E-02
Coexpression	M5957	Genes specifically up-regulated in pancreatic beta cells.	MSigDB H:	4.68E-03	2.74E-02

			Hallmark Gene Sets (v5.1)		
Coexpression	M5911	Genes up-regulated in response to alpha interferon proteins.	MSigDB H: Hallmark Gene Sets (v5.1)	5.43E-03	3.12E-02
Coexpression	M5945	Genes involved in metabolism of heme (a cofactor consisting of iron and porphyrin) and erythroblast differentiation.	MSigDB H: Hallmark Gene Sets (v5.1)	9.91E-03	4.46E-02
Coexpression	M5913	Genes up-regulated in response to IFNG [GeneID=3458].	MSigDB H: Hallmark Gene Sets (v5.1)	9.91E-03	4.46E-02

SNU761					
NAME	SIZE	ES	NES	NOM p-val	FDR q-val*
HALLMARK_PANCREAS_BETA_CELLS	40	-0.44185	-1.26291	0	1
HALLMARK_P53_PATHWAY	196	-0.40704	-1.05094	0.478088	1
HALLMARK_HEME_METABOLISM	195	-0.32601	-1.03681	0.356998	1
HALLMARK_APOPTOSIS	161	-0.42696	-1.01813	0.48583	1
HALLMARK_ADIPOGENESIS	197	-0.28875	-1.01219	0.585062	1
HALLMARK_PI3K_AKT_MTOR_SIGNALING	104	-0.27469	-0.98635	0.496855	1
HALLMARK_HYPOXIA	197	-0.42081	-0.98626	0.374741	1
HALLMARK_IL2_STAT5_SIGNALING	193	-0.33276	-0.97474	0.478088	1
HALLMARK_XENOBIOTIC_METABOLISM	199	-0.32399	-0.94012	0.567623	1
HALLMARK_UNFOLDED_PROTEIN_RESPONSE	113	-0.38885	-0.93062	0.608779	1
HALLMARK_TNFA_SIGNALING_VIA_NFKB	199	-0.51102	-0.92158	0.496894	1
HALLMARK_PROTEIN_SECRETION	96	-0.3091	-0.86077	0.689938	1
HALLMARK_IL6_JAK_STAT3_SIGNALING	87	-0.33977	-0.84897	0.374741	1
HALLMARK_KRAS_SIGNALING_UP	200	-0.30089	-0.81294	0.685484	1
HALLMARK_INTERFERON_ALPHA_RESPONSE	96	-0.3357	-0.79987	0.558704	1
HALLMARK_INTERFERON_GAMMA_RESPONSE	198	-0.30975	-0.79208	0.558704	1
HALLMARK_HEDGEHOG_SIGNALING	36	-0.39014	-0.76221	0.804436	1
*q-value is indeterminate due to batch effect in the experiment of SNU761 (see Supporting Materials and Method)					

Huh7					
NAME	SIZE	ES	NES	NOM p-val	FDR q-val
HALLMARK_HEME_METABOLISM	197	-0.38907	-1.47491	0	0.3746282
HALLMARK_UV_RESPONSE_DN	139	-0.38371	-1.46315	0	0.2413358
HALLMARK_CHOLESTEROL_HOMEOSTASIS	74	-0.56617	-1.42801	0	0.2856223
HALLMARK_BILE_ACID_METABOLISM	112	-0.42255	-1.41443	0	0.2412276
HALLMARK_HEDGEHOG_SIGNALING	36	-0.41036	-1.37465	0	0.2511859
HALLMARK_INTERFERON_ALPHA_RESPONSE	96	-0.38463	-1.31878	0	0.2870606
HALLMARK_PROTEIN_SECRETION	96	-0.26846	-1.31714	0	0.2527663
HALLMARK_INTERFERON_GAMMA_RESPONSE	199	-0.287	-1.29882	0	0.2482682
HALLMARK_KRAS_SIGNALING_DN	198	-0.31245	-1.29453	0	0.2305415
HALLMARK_FATTY_ACID_METABOLISM	156	-0.33384	-1.28244	0.102204	0.2304142
HALLMARK_GLYCOLYSIS	198	-0.31222	-1.27391	0	0.2230438
HALLMARK_ESTROGEN_RESPONSE_EARLY	194	-0.29235	-1.24387	0.10241	0.2687287
HALLMARK_MYOGENESIS	199	-0.33221	-1.23811	0	0.2554655
HALLMARK_HYPOXIA	197	-0.3144	-1.22621	0	0.2544742
HALLMARK_ANGIOGENESIS	36	-0.37356	-1.22311	0	0.2500122
HALLMARK_ANDROGEN_RESPONSE	101	-0.30373	-1.21831	0.101392	0.2461583
HALLMARK_OXIDATIVE_PHOSPHORYLATION	196	-0.27254	-1.21629	0.186373	0.2376785
HALLMARK_UNFOLDED_PROTEIN_RESPONSE	113	-0.32657	-1.16815	0.204198	0.3056852
HALLMARK_COAGULATION	138	-0.28111	-1.14519	0.10303	0.3223789

Hep3B					
NAME	SIZE	ES	NES	NOM p-val	FDR q-val
HALLMARK_FATTY_ACID_METABOLISM	156	-0.37109	-1.55336	0	0.0982857
HALLMARK_INTERFERON_GAMMA_RESPONSE	199	-0.39521	-1.4453	0	0.1401321
HALLMARK_OXIDATIVE_PHOSPHORYLATION	196	-0.25928	-1.43905	0	0.1094214
HALLMARK_ADIPOGENESIS	197	-0.34176	-1.42352	0	0.1033473
HALLMARK_XENOBIOTIC_METABOLISM	200	-0.41364	-1.40984	0	0.102335
HALLMARK_COAGULATION	138	-0.44242	-1.40753	0	0.1016602
HALLMARK_GLYCOLYSIS	198	-0.38071	-1.38192	0	0.1083618
HALLMARK_HEME_METABOLISM	197	-0.37816	-1.37867	0	0.1008165
HALLMARK_INTERFERON_ALPHA_RESPONSE	96	-0.57133	-1.37636	0	0.1005353
HALLMARK_BILE_ACID_METABOLISM	112	-0.43407	-1.36982	0	0.0952818
HALLMARK_HYPOXIA	197	-0.37422	-1.36763	0	0.0909834
HALLMARK_UNFOLDED_PROTEIN_RESPONSE	113	-0.51787	-1.34689	0	0.0999729
HALLMARK_P53_PATHWAY	196	-0.36851	-1.31934	0	0.1157463
HALLMARK_APOPTOSIS	161	-0.32587	-1.31508	0	0.1170621
HALLMARK_COMPLEMENT	199	-0.32394	-1.30434	0	0.112458
HALLMARK_PEROXISOME	102	-0.31849	-1.29135	0	0.1168692
HALLMARK_ESTROGEN_RESPONSE_LATE	200	-0.27638	-1.26833	0	0.1187342
HALLMARK_HEDGEHOG_SIGNALING	36	-0.47165	-1.24928	0.188017	0.1255351
HALLMARK_KRAS_SIGNALING_DN	198	-0.27983	-1.211	0	0.1411755
HALLMARK_KRAS_SIGNALING_UP	200	-0.28705	-1.19382	0	0.1468668

HALLMARK_ALLOGRAFT_REJECTION	200	-0.23469	-1.10182	0.210526	0.2383249
HALLMARK_APICAL_SURFACE	44	-0.27571	-1.06519	0.282744	0.2884526

HepG2					
NAME	SIZE	ES	NES	NOM p-val	FDR q-val
HALLMARK_FATTY_ACID_METABOLISM	156	-0.56096	-1.50463	0	0.180838
HALLMARK_PEROXISOME	102	-0.55796	-1.46197	0	0.2975302
HALLMARK_ADIPOGENESIS	197	-0.42836	-1.45904	0	0.2166868
HALLMARK_INTERFERON_ALPHA_RESPONSE	96	-0.52261	-1.43371	0	0.2003453
HALLMARK_HEME_METABOLISM	197	-0.44031	-1.41012	0	0.1981828
HALLMARK_ESTROGEN_RESPONSE_LATE	200	-0.43364	-1.39804	0	0.1816825
HALLMARK_ANDROGEN_RESPONSE	101	-0.33121	-1.3895	0	0.1635851
HALLMARK_BILE_ACID_METABOLISM	112	-0.58909	-1.38262	0	0.1564684
HALLMARK_INTERFERON_GAMMA_RESPONSE	199	-0.37147	-1.36553	0	0.1451941
HALLMARK_MYOGENESIS	199	-0.40534	-1.3519	0.095833	0.1609167
HALLMARK_CHOLESTEROL_HOMEOSTASIS	74	-0.60582	-1.32849	0	0.180336
HALLMARK_XENOBIOTIC_METABOLISM	200	-0.39626	-1.32226	0	0.1823531
HALLMARK_KRAS_SIGNALING_DN	198	-0.33903	-1.31653	0	0.1794663
HALLMARK_APICAL_SURFACE	44	-0.37508	-1.31321	0	0.1705758
HALLMARK_COAGULATION	138	-0.39812	-1.29086	0	0.1987224
HALLMARK_P53_PATHWAY	196	-0.35171	-1.24245	0	0.2546721
HALLMARK_ESTROGEN_RESPONSE_EARLY	194	-0.36002	-1.23562	0	0.2497135

HALLMARK_PANCREAS_BETA_CELLS	40	-0.38697	-1.21667	0.077505	0.2674183
HALLMARK_IL6_JAK_STAT3_SIGNALING	87	-0.36501	-1.21266	0.086864	0.2627938
HALLMARK_OXIDATIVE_PHOSPHORYLATION	196	-0.29689	-1.17176	0.323917	0.2980629
HALLMARK_SPERMATOGENESIS	131	-0.24363	-1.16478	0	0.2889479
HALLMARK_HEDGEHOG_SIGNALING	36	-0.36797	-1.14954	0.1125	0.2961417
HALLMARK_APICAL_JUNCTION	199	-0.3	-1.12572	0.186192	0.3201024
HALLMARK_PROTEIN_SECRETION	96	-0.22583	-1.06928	0.289225	0.4019137
HALLMARK_UV_RESPONSE_DN	139	-0.29293	-1.05526	0.371717	0.4036571
HALLMARK_PI3K_AKT_MTOR_SIGNALING	104	-0.23889	-1.02233	0.473988	0.4413551
HALLMARK_ANGIOGENESIS	36	-0.30065	-0.91592	0.482	0.6221408